TECHNISCHE UNIVERSITÄT MÜNCHEN

Lehrstuhl für Chemisch-Technische Analyse und Chemische Lebensmitteltechnologie

The influence of inhaled propylene oxide on glutathione status and cell proliferation in the respiratory nasal epithelium of rats

Mohammad Delwar Hossain Khan

Vollständiger Abdruck der von der Fakultät Wissenschaftszentrum Weihenstephan für Ernährung, Landnutzung und Umwelt der Technischen Universität München zur Erlangung des akademischen Grades eines

Doktors der Naturwissenschaften

genehmigten Dissertation.

Vorsitzender: Univ.-Prof. Dr. W. Schwab

Prüfer der Dissertation:

1. Univ.-Prof. Dr. Dr. h. c. H. Parlar
2. apl. Prof. Dr. J. G. Filser

Die Dissertation wurde am 30.10.2008 bei der Technischen Universität München eingereicht und durch die Fakultät Wissenschaftszentrum Weihenstephan für Ernährung, Landnutzung und Umwelt am 07.09.2009 angenommen.

Diese Arbeit wurde im

Institut für Toxikologie

Helmholtz Zentrum München angefertigt

und dort von Prof. Dr. J.G. Filser betreut.

I express my profound and deepest gratitude to Prof. Dr. J. G. Filser for giving me the opportunity to carry out my doctoral dissertation under his valuable guidance and supervision, for his continuous interest and encouragement in my work, and for critically evaluating this manuscript.

I am grateful and like to express my most sincere thanks to Prof. Dr. H. Parlar for being an official supervisor of my PhD work.

I sincerely thank PD Dr. Dominik Klein for his constant valuable supervision of my experimental works as well as for the correction of the manuscript.

I thank to Mrs. B. Semder and Mr. C. Pütz for their excellent technical support provided during my work.

I also take this opportunity to express my warmest thanks to all my colleagues for their constant cooperation.

My special thanks to my wife Nadera Haque who always stands beside me.

I sincerely thank to my parents, parents-in-law and my family members for their continuous encouragement.

Table of Contents

Parts of the thesis have been published

Khan M.D.H., Klein D., Quintanilla-Fend L., Oesterle D., Filser J.G. 2007. Propylene oxide induced cell proliferation in rat nasal tissue is mediated by severe perturbation of glutathione status. Naunyn-Schmiedeberg's Arch. Pharmacol. 375, 441.

Khan, M.D., Klein, D., Mossbrugger, I., Oesterle, D., Csanády, G.A., Quintanilla-Martinez, L., Filser, J.G. 2009. Is propylene oxide induced cell proliferation in rat nasal respiratory epithelium mediated by a severe depletion of water-soluble non-protein thiol? Toxicol. Lett. 185, 203-210.

TO

MY FAMILY

1 INTRODUCTION

1.1 Objective

Propylene oxide (1,2-epoxypropane, methyloxacyclopropane; PO) is an important industrial chemical used for the production of plastics and other synthetic materials. The main route of human exposure to PO occurs by inhalation at the workplace. The International Agency for Research on Cancer classified PO as *possibly carcinogenic to humans* (IARC, 1994).

In rodents, PO is a site of contact carcinogen after long-term exposures. Local tumors were induced after sc injections and tumors in the forestomach of female Sprague-Dawley rats and NMRI mice after exposures by oral gavage (Dunkelberg, 1981, 1982). Fischer 344 rats and B6C3F1 mice exposed to PO by inhalation developed tumors in the nasal cavity, rats at PO concentrations ≥300 ppm and mice at 400 ppm (Lynch et al., 1984; Renne et al., 1986). Although differences in tumorigenic response were noticed between rodent species and strains, histopathological examination of the nasal tissue demonstrated that tumor formation was accompanied by cytotoxic and hyperplastic changes in the nasal cavity in both species. Such lesions were minimal or absent in animals exposed to lower PO concentrations and in controls (Lynch et al., 1984; Renne et al., 1986; Kuper et al., 1988). PO was mutagenic in microorganisms and in Drosophila, mutagenic and clastogenic in mammalian cells in vitro (reviewed in IARC, 1994; Kolman et al., 2002), and clastogenic at very high doses in vivo in mice (300 and 450 mg/kg, ip administration, Bootman et al., 1979; Farooqi et al., 1993) and in Drosophila (≥1000 ppm, inhalation: Vogel and Nivard, 1998).

PO directly reacts with DNA forming mainly the N7-(2-hydoxypropyl) guanine (N7-HPG) adduct (Plná et al., 1999; Solomon et al., 1988). Studies in vivo revealed higher N7-HPG concentrations in rat respiratory nasal epithelium

(RNE) than in other tissues after inhalation exposure (Ríos-Blanco et al., 1997, 2000; Segerbäck et al., 1998) in agreement with a higher intracellular PO concentration in RNE calculated by a physiological toxicokinetic model (Csanády and Filser, 2007).

The PO concentration-dependent increase in N7-HPG adducts in RNE after inhalation exposure to PO for 3 or 20 days (6 h/day, 5 days/week) correlated almost linearly with the concentration of PO. However, it did not parallel the exposure response for tumor formation (Ríos-Blanco et al., 2003a). The observation that tumors in RNE developed only when inflammatory lesions and cell hyperplasia were present, suggest that PO induced nasal tumorigenicity does not result solely from the genotoxicity of PO.

Studies with rats revealed that inhalation exposure to ≥300 ppm PO for 3 days (6 h/day) and up to 4 weeks (6 h/day, 5 days/week) resulted in statistically significantly increased cell proliferation in RNE (Eldridge et al., 1995; Ríos-Blanco et al., 2003b). Lee et al. (1998, 2000, 2005) demonstrated in PO exposed rats an inverse correlation between cell proliferation in RNE and the glutathione (GSH) content in this tissue, measured as water-soluble non-protein thiol (NPSH). Also, in isolated upper respiratory tracts of mice a PO concentration dependent decrease of NPSH was demonstrated (Morris and Pottenger, 2006; Morris et al., 2004). As was shown by the physiological toxicokinetic model of Csanády and Filser (2007), the PO dependent GSH depletion in RNE is caused by the imbalance between the rapid conjugation of GSH with PO in RNE (a reaction investigated by Faller et al., 2001) and the slow GSH turnover in this tissue. In agreement with earlier observations demonstrating a linkage between perturbation of the GSH status and cell proliferation (reviewed in, e.g., Burdon, 1995), Lee et al. (2005) hypothesized a repeated and severe perturbation of the GSH levels, resulting from the

metabolic PO elimination by GSH conjugation, to be the molecular cause of the PO induced cell proliferation in rat RNE. The goal of the present study was to investigate this hypothesis by means of different approaches. First, cell proliferation and NPSH status in RNE were studied upon exposing groups of male Fischer 344 rats over 3 days by inhalation to PO concentrations between 50 and 300 ppm. Second, it was tested whether PO induced NPSH depletion and cell proliferation in RNE could be prevented by simultaneously administering the GSH precursor N-acetylcysteine (NAC). Third, rats were treated for three days with different doses of the GSH depleting agents diethylmaleate (DEM) and L-buthionine sulfoximine (BSO) in order to study whether NPSH depletion as such can result in cell proliferation in RNE.

1.2 Properties of propylene oxide

1.2.1 Physico-chemical properties, production, and use

PO is a highly volatile, clear, colorless, extremely flammable liquid with an ether-like odor (IARC, 1994). Its molecular weight is 58.1 g, its melting point is -112°C, and its boiling point is 34°C at 760 mm Hg (EC, 2002). PO has a water-to-air partition coefficient of 78, and a blood-to-air partition coefficient of 60 at 37°C (Schmidbauer et al., 1997). It is soluble in water and fully miscible with acetone, benzene, carbon tetrachloride, diethyl ether, and ethanol.

Worldwide production of PO exceeds four million tons per year (Zuwei et al. 2001). Large volume producers are found in Japan, the USA, and Western Europe (IARC, 1994). PO is used primarily to produce polyether polyols, propylene glycols and propylene glycol ethers. PO is also used for the synthesis of various special organic compounds like allyl alcohol, propylene carbonate, mono-, di-, and tri-isopropanolamins and hydroxypropylated cellulose.

Hydroxypropyl starch ethers, produced by treating starch with PO, are used as additives in salad dressings, pie fillings and food thickening applications. In addition, PO has limited use as a fumigant for dried fruits, nuts, species, cocoa, processed nutmeats, starch and gums and as reactive diluent in preparations for embedding tissues for transmission electron microscopy (summarized in IARC, 1994).

1.2.2 Exposure and regulations

The primary route of potential human exposure to PO is inhalation at the workplace during the production of polyurethane polyols and propylene glycol. The American National Occupational Exposure Survey, conducted between 1981 and 1983, estimated that 421000 employees in the United States were potentially exposed to PO (cited in IARC, 1994). Exposure of the general population may occur through ingestion of PO residues in foods or by contact with consumer products containing PO. The American Conference of Governmental Industrial Hygienists set a threshold limit value of 2 ppm PO for workplace exposures (ACGIH, 2008).

1.2.3 Adverse effects

Genotoxicity

PO is a monoalkylating DNA-reactive agent reacting preferentially with cyclic ring nitrogens in DNA. In agreement, different DNA adducts were detected after incubation of PO with salmon sperm DNA (Lawley and Jarman, 1972) or calf thymus DNA (Djuric et al., 1986; Randerath et al., 1981; Solomon et al., 1988). In rats and mice, upon PO inhalation exposure, PO adducts with DNA

have been detected in all tissues investigated (Osterman-Golkar et al., 2003; Ríos-Blanco et al., 1997, 2003a; Segerbäck et al., 1994, 1998; Snyder and Solomon, 1993; Svensson et al., 1991). The highest PO adduct levels were found in RNE, with up to 25-fold higher than in other, systemically exposed tissues (Osterman-Golkar et al., 2003; Ríos-Blanco et al., 1997, 2003a; Segerbäck et al., 1998). The most abundant PO-DNA adduct in RNE of rats exposed to 500 ppm PO for 4 weeks (6h/day, 5 days/week) was N7-HPG followed by adducts with N1 and N^6 of adenine (N1-HPA, N^6-HPA; together ~ 2% relative to N7-HPG) and N3 of uracil (N3-HPU; ~ 0.02% relative to N7-HPG; Plná et al., 1999). N7-HPG was also the predominant adduct after incubation of PO with calf thymus DNA (Solomon et al., 1988). The different PO-DNA adducts are considered to have different mutagenic potencies: N7-HPG is regarded to be a non-promutagenic lesion since it does not distort DNA structure or lead to ring-open transformations. In contrast, N1-HPA, N^6-HPA, and N3-HPU are considered to be promutagenic (Albertini and Sweeney, 2007).

Mutagenicity of PO was extensively investigated in bacteria and mammalian cells in vitro (for reviews see Albertini and Sweeney, 2007; Giri, 1992; IARC, 1994; Kolman et al., 2002). In both systems, PO caused DNA damage and gene mutations. Gene mutations were also detected in yeast and fungi. In mammalian cells including human lymphocytes in vitro, sister chromatid exchange and chromosomal aberrations were found. PO was also positive in neoplastic cell transformation tests.

In *Drosophila*, significant induction of sex-linked recessive lethal mutations and chromosomal aberrations were observed after PO inhalation exposures (Hardin et al., 1983; Vogel and Nivard, 1997, 1998).

In mammals in vivo, mutagenicity studies have examined events on the chromosome level; gene mutations have not been assessed. Regarding

chromosomal abnormalities or micronuclei in bone marrow cells, ip injection of PO to male and female mice (females: five dosage of up to 450 mg/kg each; males: two dosages of up to 300 mg/kg each) gave positive results (Bootman et al., 1979; Farooqi et al., 1993) whereas administration by oral gavage (male mice, two dosages of up to 500 mg/kg each; Bootman et al., 1979) or by inhalation (cynomolgus monkeys up to 300 ppm, 7 h/day, 5 days/week for 2 years; Lynch et al., 1984a) gave negative results. Regarding germ cells, dominant lethal tests in male mice after PO treatment by oral gavage up to 250 mg/kg/day for 14 days or in male rats after PO inhalation exposure to 300 ppm for 5 days (7 h/day) were negative (Bootman et al., 1979; Hardin et al., 1983).

In humans exposed to PO, adducts with DNA (Czène et al., 2002) and hemoglobin (Ball et al., 2005; Boogaard et al., 1999; Czène et al., 2002; Jones et al., 2005; Pero et al., 1985) have been reported.

It should be noted that the genotoxic potency of PO is low as compared to other mononucleating chemicals as has been shown with epichlorohydrin (Kolman et al., 1997) or with ethylene oxide, both in vivo (Farooqi et al., 1993; Högstedt et al., 1990; Lynch et al., 1984a; Vogel and Nivard, 1997, 1998) and in vitro (Agurell et al., 1991).

Irritation and skin sensitization

Under non-occlusive conditions, concentrated PO did not show irritant effects on the skin because of fast evaporation. Aqueous solutions with less than 10% PO are highly irritative to skin and mucous membranes and can even cause corrosion. Eye irritancy has been described upon contact with vaporous or aqueous PO (Hine et al., 1981; Carpenter and Smyth, 1946; McLaughlin, 1946). Allergic contact dermatitis was diagnosed in 4 cases of exposure to solutions of

PO (Jensen, 1981; Steinkraus and Hausen, 1994; van Ketel, 1979).

Acute toxicity

The LD50 for rats was 523 mg/kg (0.63 ml/kg) after single oral administration of PO, (Weil et al., 1963). In two studies, oral LD50s for rats were 946 mg/kg and 520 mg/kg for males, and 540 mg/kg for females (cited in WHO, 1985). For male mice and guinea pigs, oral LD50s were 630 and 660 mg/kg respectively (cited in WHO, 1985). The LC50 upon inhalation exposure (4 h) was 4000 ppm PO and 1740 ppm PO for male rats and mice, respectively (Jacobson et al., 1956). In rats exposed by inhalation to 4000 ppm PO for 0.5 h, to 2000 ppm PO for 2 h, or to 1000 ppm PO for 7 h, no organ injury was observed (Rowe et al., 1956).

Subacute and subchronic toxicity

In rats, Guinea pigs, rabbits, and monkeys exposed to 100 and 200 ppm PO for 5 days (7 h/day), no effects were found with the exception of slightly increased lung weights in female Guinea pigs at 200 ppm. In another study, young female rats were orally treated 5 times per week (in total 18 times) with PO doses of 0.1, 0.2, and 0.3 g/kg. Decreased body weights, irritation of the gastric mucosa, and slight liver injury were observed at the highest dose group. In an inhalation study with rats of both genders (75, 150, 300, and 600 ppm PO; 6 h/day, 5 days/week, 13 weeks) decreased body weight development and slightly degenerative and hyperplastic changes of the nasal epithelium occurred at the highest dose. All studies are summarized in DFG (1996).

Male Fischer 344 rats were exposed to 0, 10, 20, 50, 150 or 525 ppm PO (6 h/day, 5 days/week) for 1 or 4 weeks followed by four weeks of recovery. Toxicity and cell proliferation were examined in the nasal cavity of control and exposed rats.

At ≤50 ppm PO, no effects were detected. At 525 ppm PO, respiratory epithelial hyperplasia, degeneration of the olfactory epithelium, and cell proliferation at both sides of the nasal cavity were observed. These changes were most pronounced immediately after termination of the exposure. The effects were reversible (Eldridge et al., 1995). Another study with male Fischer 344 rats exposed to 0, 5, 25, 50, 300, or 500 ppm PO (6 h/day, 5 days/week, 4 weeks; Lee et al., 2005) and 0 or 500 ppm PO (6 h/ day, 5 days/week, 4 weeks; Ríos-Blanco et al., 1997) revealed reduced body weight development at 500 ppm PO after 2 weeks. Furthermore, PO inhalation exposure (0, 5, 25, 50, 300, or 500 ppm; 6 h/day) of male Fischer 344 rats for 3 or 20 days (5 days/week) resulted in statistically significant increased cell proliferation in RNE at ≥300 ppm PO (Ríos-Blanco et al., 2003b). Inhalation exposure of male Wistar rats to 1500 ppm PO for 7 weeks (6 h/day, 5 days/week) caused ataxia in the hind legs (Ohnishi and Murai, 1993).

Chronic toxicity and carcinogenicity

Male Fischer 344 rats were exposed to 0, 100, or 300 ppm PO (7 h/day, 5 days/week) for 140 weeks. As compared to the control group, the mean body weights of the 100 and 300 ppm groups were significantly lower from exposure week 39 and 2, respectively. Significant increase in mortality and skeletal muscle atrophy were observed at 300 ppm PO. At both PO concentrations, increased incidences of inflammatory lesions in the nasal cavity, trachea, lung and middle ear were found. A dose-dependent increase in the incidence of epithelial hyperplasia was observed in the nasal mucosa (statistically significant at 300 ppm PO). Two rats in the 300 ppm group developed adenomas in the nasal cavity, which were absent in controls. Adrenal phaeochromocytomas developed non dose-dependently in 10% of controls, 32% of rats at 100 ppm PO

and 27% of rats at 300 ppm PO. After about 16 months of exposure, an outbreak of Mycoplasma pulmonis infection affected all animal groups. The infection was discussed to have influenced survival and lesions in lungs, middle ear and nasal passages (Lynch et al., 1984).

In another study, male and female Fischer 344 rats and male and female B6C3F1 mice were exposed by inhalation to 0, 200, or 400 ppm PO (6 h/day, 5 days/week) for 103 weeks. At 400 ppm PO, mean body weights of mice of both sexes and male rats were decreased during the 2nd year of exposure. At terminal sacrifice, mean body weights of male and female rats exposed to 400 ppm PO were within 10% of the control values. Survival of mice of both sexes exposed to 400 ppm PO was significantly decreased. Among rats, no statistically significant differences in survival were observed. In both species and both sexes, a dose-related increase in rhinitis was seen at both PO concentrations. In rats exposed to 400 ppm PO, there were significant increases of squamous metaplasia and hyperplasia in the RNE. Papillary adenomas of the nasal cavity occurred in 0% of controls, in 0% at 200 ppm PO, and in 6% (females) and 4% (males) at 400 ppm PO. In the nasal cavities of mice, statistically significant increases in hemangiomas and hemangiosarcomas were found in the highest dose group of 400 ppm PO (Renne et al., 1986).

After inhalation exposure of Wistar rats of both genders (6 h/day, 5 days/week, up to 124 weeks) to 0, 30, 100, or 300 ppm PO, mortality was increased in females at 100 ppm PO by week 119 and in both sexes at 300 ppm PO by week 115. As compared to controls, body weights were significantly lower at 300 ppm PO, in females during the first year and in males throughout the study. Three male animals developed nasal tumors: one ameloblastic fibrosarcoma and one squamous cell carcinoma among 61 animals at 30 ppm PO and one squamous cell carcinoma among 63 animals at 300 ppm PO. None of these

neoplasms were considered to be compound related because of similar incidences in the historical control group. Increased degenerative and hyperplastic changes in the nasal mucosa were reported in all treatment groups. In addition incidences in benign and malign mammary gland tumors were significantly higher in female rats at 300 ppm PO. Their relevance was doubted because within the historical control incidence in this laboratory. Additionally, in 4 out of 63 male rats of the 300 ppm group, carcinomas were detected in the larynx/pharynx, trachea, or lung. No such tumor was seen in any of the rats exposed to 0 or 30 ppm PO (Kuper et al., 1988). Groups of 100 female NMRI mice received sc injections of PO dissolved in tricaprylin (1,2,3-trioctanoylglycerol) at doses of 0.1, 0.3, 1.0 or 2.5 mg/mouse once a week for 95 weeks. Groups of 200 untreated and 200 tricaprylin-treated mice served as controls. Survival rates in the PO treated animals were similar to those in controls. The incidences of sarcoma at the site of injection were: control: 0%; tricaprylin treatment: 2%; 0.1 mg PO: 3%; 0.3 mg PO: 2%; 1.0 mg PO: 12%, and 2.5 mg PO: 15%. No increase in tumor incidence was found at other sites (Dunkelberg, 1981).

Upon intragastric administration of PO to Sprague–Dawley rats (0, 15, 60 mg/kg; 2 doses per week; 109.5 weeks), the survival rates of the treated rats were similar to those of the control groups. Tumors developed dose-dependently in the forestomach of the PO treated rats. Control animals did not develop any forestomach tumors (Dunkelberg, 1982).

In another PO study, twelve rats were given a total dose of 1500 mg/kg PO in peanut oil by sc injection over a period of 325 days. No information was provided regarding the frequency of doses, the doses per application and the animal sex. Local sarcomas were developed in eight rats after 507-739 days. When the same dose was administered in water as vehicle, 25% of the rats

developed local sarcomas after 158 days and 17% developed local sarcomas after 737 days (Walpole, 1958).

Concerning human carcinogenicity data on PO, there are some cohort studies in workers who were exposed mainly to ethylene oxide. Some of these workers were also exposed to PO. In addition, one case-control study was conducted in workers who were exposed to PO and 20 other chemicals. None of these studies enabled to draw any conclusion about a PO related carcinogenic risk to humans (summarized in IARC, 1994).

In summary, PO induced tumors in rodents mainly at the application site. Upon inhalation exposure of rats, tumors developed in the nasal mucosa. A revision of the slides from the rat carcinogenicity bioassay (Renne et al., 1986) demonstrated all nasal adenomas to be located adjacent to the transitional epithelium lining the ventral lateral surface of the nasoturbinates (Ríos-Blanco et al., 2003b). Taking into consideration the information on genotoxicity, rodent carcinogenicity together with the inadequate human carcinogenicity data, the International Agency for Research on Cancer classified PO as *possibly carcinogenic to humans* (IARC, 1994).

1.2.4 Metabolism

Inhaled vaporous PO was effectively metabolized in rats. Only a fraction of 3% was exhaled unchanged (Golka et al., 1989). Studies in microsomes and cytosol revealed PO hydrolysis to be catalyzed by epoxide hydrolase (EH; Faller et al., 2001; Guengerich and Mason, 1980) and its glutathione conjugation by glutathione S-transferase (GST; Faller et al., 2001; Fjellstedt et al., 1973). Hydrolsis of PO by EH leads to 1,2-propanediol which is either excreted unchanged or enters the intermediary metabolism after oxidation to lactic acid and pyruvic acid (cited in Ruddick, 1972). The GSH conjugates of PO are

further metabolized to mercapturic acids (Fjellstedt et al., 1973) which are urinary excreted (Figure 1). As a direct alkylating agent, PO binds to macromolecules forming hydroxypropyl adducts with DNA (see above) and with proteins such as hemoglobin (Bailey et al., 1987; Boogaard et al., 1999; Czène et al., 2002; Farmer et al., 1982; Högstedt et al., 1990; Jones et al., 2005; Osterman-Golkar et al., 2003; Pero et al., 1985; Ríos-Blanco et al., 2002; Svensson et al., 1991). The investigated hemoglobin adducts were those with histidine-N, cysteine-S, and the amino group of the N-terminal valine (Svensson and Osterman-Golkar, 1984; Segerbäck et al., 1994).

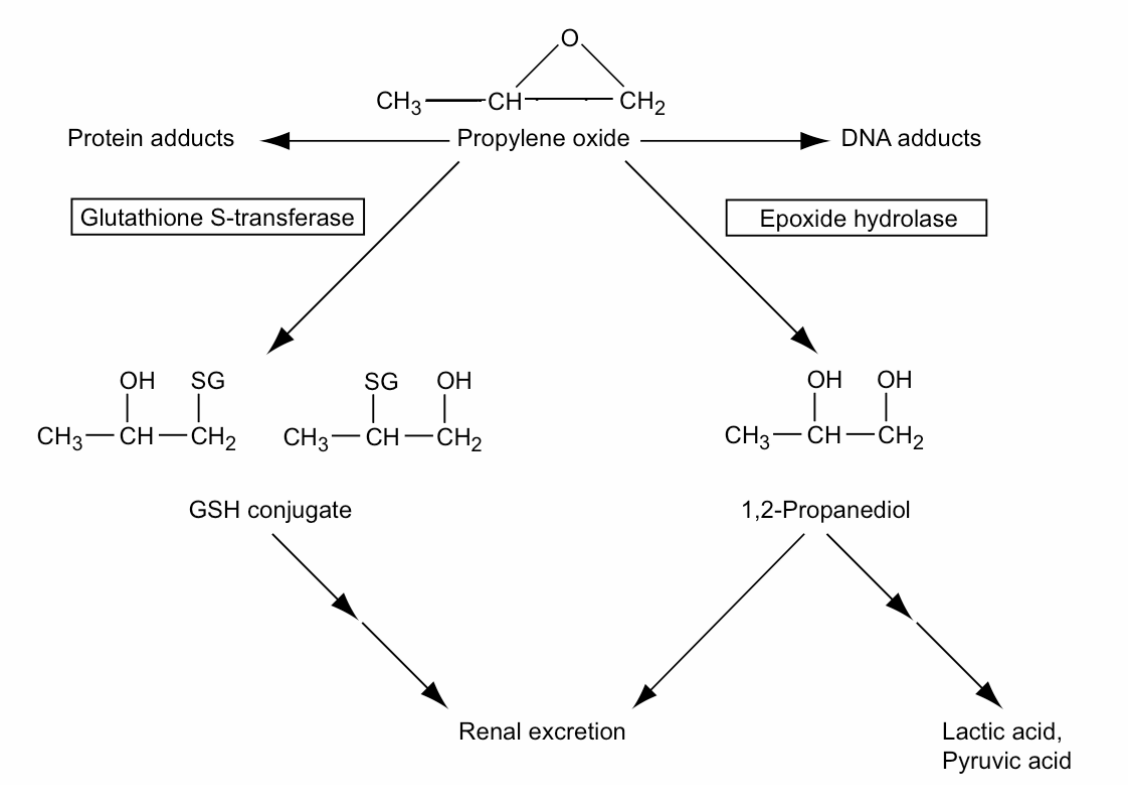

Figure 1: Metabolism of propylene oxide.

1.3 Glutathione: biological role and relevance in propylene oxide exposure

GSH is a tripeptide consisting of glutamate, cysteine and glycine that contains a γ-peptide bond between glutamate and cysteine. GSH is the most abundant intracellular thiol with tissue specific concentrations of 0.2-10 mmol/l. It is synthesized in the cytosol in two steps. The first and rate limiting reaction is the formation of γ-glutamylcysteine, catalyzed by γ-glutamycysteine synthetase. In the second step, catalyzed by GSH synthetase, GSH is formed from γ-glutamylcysteine and glycine. GSH is involved in a multitude of cellular functions (summarized e.g. in: Anderson et. al., 1998; Comporti, 1989; DeLeve and Kaplowitz, 1991; Pompella et al., 2003). One of the major functions of GSH is to protect cells against oxidative damage by maintaining the intracellular redox state. GSH functions as a redox equivalent during its enzymatic oxidation catalyzed by the GSH peroxidase with co-substrates such as hydrogen peroxide and lipid peroxides. During this reaction, hydrogen peroxide and lipid peroxides are reduced to water and alcohols, respectively. The oxidized product of GSH, the GSSG dimer, is again reduced to GSH by GSH reductase under the consumption of NADPH as co-substrate. GSH plays also an important role in the metabolic elimination of electrophilic xenobiotics. It can be conjugated by GSTs to such compounds thereby facilitating their excretion from the organism. The consumption of intracellular GSH depends primarily on oxidative stress and metabolism of xenobiotics. If the consumption of GSH exceeds its re-synthesis, an intracellular decline of the GSH level will result. The GSH status, determined as NPSH, was investigated in blood, livers, lungs, and RNE of rats exposed repeatedly (6 h/day) for up to 4 weeks (5 days/week) to PO concentrations of 0, 5, 25, 50, 300, and 500 ppm. NPSH levels were determined immediately at the end of the exposures. With increasing PO concentrations,

NPSH levels decreased in blood marginally, but reached in livers and lungs at 500 ppm PO about 50% and 67%, respectively, of the corresponding control levels. The most distinct concentration-dependent NPSH depletion was observed in RNE with minimum levels of about 25% of the control levels at 300 and at 500 ppm PO (Lee et al., 2005). This minimum reflected almost complete loss of GSH, because NPSH in RNE consists to about 76% of GSH (Potter et al., 1995). The decline of cellular GSH was demonstrated by means of a physiological toxicokinetic model to result from GST mediated PO conjugation with GSH: During exposures to high PO concentrations, GSH conjugation led tissue-specifically to a loss of GSH as a consequence of a slower rate of replenishment of the GSH pool if compared to the PO conjugation rate (Csanády and Filser, 2007).

Depletion of GSH can lead to cytotoxicity (reviewed in, e.g. Comporti, 1989), apoptosis (reviewed in, e.g. Cotgreave and Gerdes, 1998; Slater et al., 1995) and cell proliferation (reviewed in, e.g. Burdon, 1995). In the rats, exposed to 300 and 500 ppm PO, the end-exposure NPSH levels were discussed to be low enough for such effects in RNE (Lee et al., 2005). Accordingly, a statistically significant increase in cell proliferation in RNE of rats repeatedly exposed to PO (6 h/day, 3 days or 6 h/day, 5 days/week, up to 4 weeks) was observed at concentrations of 300, 500, and 525 ppm (Eldridge et al., 1995; Ríos-Blanco et al., 2003b).

1.4 Aim of the study

Combining the findings on PO dependent tumor incidences, DNA adducts, genotoxicity, NPSH status and cell proliferation in RNE as well as on metabolism and kinetics of PO in RNE, Lee et al. (2005) proposed a mode of action for PO induced nasal tumorigenicity. The authors hypothesized a

repeated and severe perturbation of GSH levels – resulting from metabolic PO elimination by GSH conjugation – to be the molecular cause of PO induced cell proliferation and the latter to be a critical step on the path to tumors in rat RNE. This mechanism, when substantiated, could serve as a starting point for the estimation of the carcinogenic risk to humans from exposure to PO.

The aim of the present study was to provide experimental evidence to corroborate the hypothesized link between GSH status and cell proliferation by means of different approaches. First, cell proliferation and NPSH status in RNE were studied upon exposing groups of male Fischer 344 rats over 3 days by inhalation to various PO concentrations. Second, it was tested whether PO induced NPSH depletion and cell proliferation in RNE could be prevented by administering the GSH precursor NAC. Finally, rats were treated for three days with different doses of the GSH depleting agents DEM and BSO in order to study whether NPSH depletion as such can result in cell proliferation in RNE.

2 MATERIALS AND METHODS

2.1 Materials

Chemicals

Ammonium acetate, 99.9%	Sigma-Aldrich, Steinheim, Germany
5-Bromodeoxyuridine, 99%	Sigma-Aldrich, Steinheim, Germany
Carbon dioxide	Linde, München, Germany
Diethylmaleate, 97%	Sigma-Aldrich, Steinheim, Germany
Disodium ethylenediaminetetraacetate dihydrate, ~99%	Merck, Darmstadt, Germany
5,5'-Dithiobis-(2-nitrobenzoic acid), 99%	Sigma-Aldrich, Steinheim, Germany
Eosin Y, Microscopy	Merck, Darmstadt, Germany
Ethanol, 99.9%	Merck, Darmstadt, Germany
Ether, 99+%	Sigma-Aldrich, Steinheim, Germany
Ethylenediaminetetraacetic acid, 99%	Roth, Karlsruhe, Germany
Fluimucil® (N-acetylcysteine) injection solution, 10%	Zambon, Kerpen, Germany
Formaldehyde, 37%	Roth, Karlsruhe, Germany
Glutathione, reduced, 99.9%	Sigma-Aldrich, Steinheim, Germany
Goat serum, GIBCO™	Invitrogen, Auckland, New Zealand
Hematoxylin, Microscopy	Merck, Darmstadt, Germany
Hexane PESTANAL®	Riedel-de-Haën, Seelze, Germany
Hydrochloric acid, 32%	Merck, Darmstadt, Germany
Hydrogen 5.0	Linde, München, Germany

iVIEW™ DAB detection kit	Ventana Medical System, Tucson, AZ, USA
Isofluorane (Isoba®)	Essex Tierarznei, München, Germany
L- Buthionine sulfoximine, ≥97%	Sigma-Aldrich, Steinheim, Germany
Liquid nitrogen	Linde, München, Germany
Metaphosphoric acid, 65%	Merck, Darmstadt, Germany
Methanol, 99.9%	Merck, Darmstadt, Germany
Monoclonal mouse anti-bromodeoxyuridine, clone Bu20a	DAKO, Carpinteria, CA, USA
Nitrogen 5.0	Linde, München, Germany
Olive oil (Grade: Ph Eur)	Sigma-Aldrich, Steinheim, Germany
Potassium carbonate, 99.5%	Merck, Darmstadt, Germany
Potassium phosphate, dibasic, 99.5%	Merck, Darmstadt, Germany
Potassium phosphate, monobasic, 99.5%	Merck, Darmstadt, Germany
Propylene oxide, 99.99%	Lyondell, Rotterdam, The Netherlands
Pursept®-A	Merz, Frankfurt, Germany
Saline (Isotonic solution of sodium chloride)	B. Braun, Melsungen, Germany
Soda lime, Drägersorb® 800	Drägerwerk, Lübeck, Germany
Sodium bicarbonate, 99%	Merck, Darmstadt, Germany
Sodium chloride, 99.5%	Merck, Darmstadt, Germany
Sodium hydroxyide pellets, 99%	Merck, Darmstadt, Germany
Synthetic air	Linde, München, Germany
Tris(hydroxymethyl) aminomethane, Trizma® base, 99.9% titration	Sigma-Aldrich, Steinheim, Germany
Trisodium citrate dihydrate, ≥99%	Merck, Darmstadt, Germany

Tween® 20, ≥99%	Sigma-Aldrich, Steinheim, Germany
Xylene, ≥99%	Merck, Darmstadt, Germany

Instruments

Alzet osmotic pumps (2ML)	DURECT Corp, Cupertino, CA, USA
Analytical balance (A 210-P)	Sartorius, Göttingen, Germany
Automated immunostainer, NexEs® IHC	Ventana Medical System, Tucson, AZ, USA
Blood gas critical care analyzer, STAT Profile pOHx	NOVA Biomedical, Rödermark, Germany
Centrifuge Biofuge B	Haraeus Sepatech, Osterode, Germany
Centrifuge Sigma 4K10	Sigma, Osterode, Germany
Evaporator for isoflurane, TEC 3	Ohmeda, Steeten, England
Gas Chromatograph GC-8A equipped with	Shimadzu, Duisburg, Germany
Flame ionization detector	
Integrator, C-R5A Chromatopac	
Stainless steel column packed with Tenax TA, 60-80 mesh, 2.5 m x 1/8″ x 2 mm	Varian, Darmstadt, Germany
Light Microscope AXIOPLAN equipped with	Zeiss, Jena, Germany
uEye® USB 2.0 camera	SDT Dr. Steiner, Seefeld, Germany
Magnetic Stirrer, M5 CAT	M. Zipperer, Staufen-Etzenbach, Germany

Microplate Reader, SPECTRA MAX 340	Molecular Devices, München, Germany
Microtom (HM 355)	Microm, Walldorf, Germany
Potter Homogenizer equipped with teflon glass cylinder and plunger, 2 ml	B. Braun, Melsungen, Germany B. Braun, Melsungen, Germany
pH meter, Knick 646	Knick, Berlin, Germany
pH-Electrode In lab®	Mettler Toledo, Urdorf, Switzerland
Stereo microscope Stemi SV11 equipped with cold light source KL 1500 electronic	Zeiss, Jena, Germany
UV/VIS spectrophotometer, Lambda 5	Perkin Elmer, Überlingen, Germany
Ultrasonicator, Sonorex TK 30	Bandelin Electronics, Berlin, Germany
Vacuum infiltration processor, Tissue-Tek®,VIP™	Vogel, Gießen, Germany
Vortex VF2	Janke & Kunkel, Staufen, Germany

Laboratory ware

Absorbent protector sheets, polythene backed (Whatman®)	Whatman International, Maldstone, England
Adhesive tape	Neolab, München, Germany
Base plate, polypropylene	Helmholtz Center München, Neuherberg, Germany
Beaker, glass, 100, 300, and 5000 ml	Schott Duran, Mainz, Germany

BD Falcon™ conical and round bottom tubes, 15 and 50 ml	BD Biosciences, Heidelberg, Germany
Cuvets, suprasil®, glass, 1.8 ml thickness 1.0 cm	Perkin Elmer, Überlingen, Germany
Desiccator, glass, 6 l	Glaswerk Wertheim, Germany
Eppendorf-cups, 1.5 and 2.0 ml	Eppendorf, Hamburg, Germany
Exposure chamber, glass, 64 and 68 l	Kuglstatter, Garching, Germany
Flange seal and clamp	Schott Duran, Mainz, Germany
Flask, glass, conical, 5000 ml	Schott Duran, Mainz, Germany
Funnel, glass, diameter 14.5 cm	Schott Duran, Mainz, Germany
Grease (Silicon-free, Glisseal HV)	Borer Chemie, Zuchwil, Switzerland
Hamilton syringe, gas tight, 5, 100, and 1000 µl	Hamilton, Bonaduz, Switzerland
Icebath	Neolab, München, Germany
Laboratory glass bottles with screw caps, Duran®, 100 and 500 ml	Schott Duran, Mainz, Germany
Magnetic fish	Bohlender, Lauda, Germany
Measuring cylinder, glass, 10, 50, and 2000 ml	Schott Duran, Mainz, Germany
Needle, disposable, 0.90 x 40 mm, 0.45 x 12 mm, and 1.20 x 40 mm	B. Braun, Melsungen, Germany
Microplate (Nunc™ 96-well)	Nunc A/C, Rosklide, Denmark
Pasteur pipettes, soda lime glass, disposable, long and fine tip, 10 and 20 mm	Hirschmann, Eberstadt, Germany
Pertex®	Medite Medizintechnik, Burgdorf, Germany

Plastic screw caps, GL 14	Schott Duran, Mainz, Germany
Pipettes with adjustable different volumes	Eppendorf, Hamburg, Germany
Pipette “epTIPS”, different volumes	Eppendorf, Hamburg, Germany
Preparation table for rats	Hugo Sachs Electronik, Harvard Apparatus, March-Hugstetten, Germany
Septa CS, teflon coated silicone	SGE, Griesheim, Germany
Slides, SuperFrost® Plus, Microscope slides	Menzel-Gläser, Braunschweig, Germany
Syringes, Omnifix-F Solo, disposable, 1, 3 and 10 ml	B. Braun, Melsungen, Germany
Surgical instruments	Aesculap, Tuttlingen, Germany
Thread tape, PTFE	Carl Roth, Karlsruhe, Germany
Thermometer (-10°-110°C)	Amarell, Kreuzwertheim, Germany
Timer	Oregon Scientific, Neu-Isenburg, Germany

Computer and printer

Apple Macintosh, iMac	Apple, Cupertino, CA, USA
EPSON, EPL-N 3000	EPSON, Hemel Hempstead, UK

Software

Adobe Illustrator 10.0	Adobe Systems, San Jose, CA, USA

CS ChemOffice 2002	CambridgeSoft®,Cambridge, MA, USA
EndNote 6.0	Thomson Research Soft, Carlsbad, CA, USA
Microsoft Office 2004	Microsoft, Redmond, WA, USA
NexES IHC 750-011	Ventana Medical System, Tucson, AZ, USA
Optimas image analysis software, 6.51	Optimas Corporation™, Bothell, WA, USA
Sigma Plot 10.2	Jandel, Erkrath, Germany

2.2 Animals

Male Fischer 344 rats (Charles River, Sulzfeld, Germany) with body weights of 230-260 g at start of the experiments were used in all studies. Animals were housed in Macrolon cages (3 animals/cage) and provided with HEPA-filtered air in a TOP FLOW-IVC-system (Tecniplast, Buggugiate, Italy). The animal room air was cleaned of particles by active charcoal filters and maintained at 23°C and 40-60% relative humidity. A constant light–dark cycle with light from 7:00 to 19:00 h was kept. Rats were provided food (Standard chow 1324, Altromin, Lage, Germany) and tap water ad libitum except during the inhalation exposure periods. Body weights were recorded at the time of arrival and daily during the treatment periods. Animals were assigned randomly to the different treatment groups and were observed daily for overt signs of toxicity. Treatments of rats were done in agreement with the German Animal Welfare Law.

2.3 Methods

2.3.1 Gas chromatography of propylene oxide

PO concentrations in the atmosphere of the exposure chamber were determined using a gas chromatograph (GC; type GC-8A) equipped with a flame ionization detector (FID).

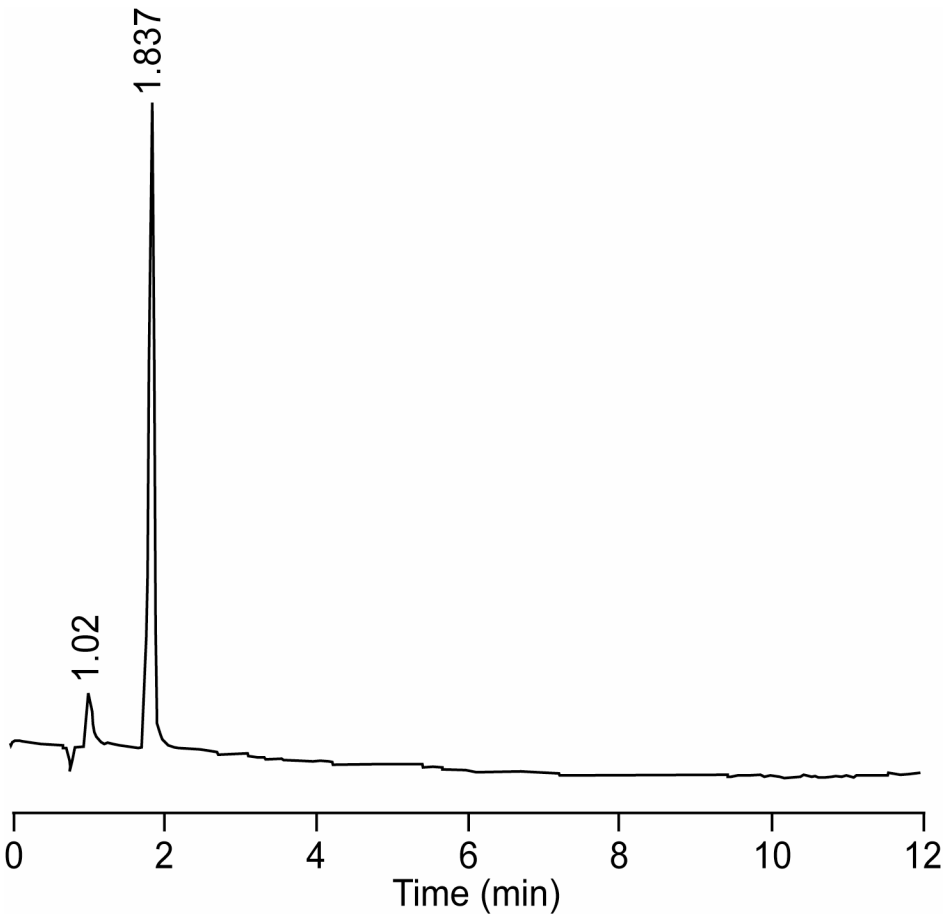

Figure 2: Typical gas chromatogram of propylene oxide (PO) in the atmosphere of the animal exposure chamber.
PO concentration: 50 ppm; injection volume: 50 µl; retention time: 1.837 min.
GC conditions: range 1; attenuation 3.

Gas samples of 50 µl were taken by means of a gas tight syringe through a teflon-coated rubber septum and were injected direct on-column via the heated

GC injector (210°C). Separations were done isothermally at 160°C on a stainless steel column packed with Tenax TA. Nitrogen was used as carrier gas with a pressure of 3.0 kg/cm². The detector was kept at 210°C and was supplied with hydrogen (0.7 kg/cm²) and synthetic air (0.7 kg/cm²). Areas under the peaks (retention time 1.8 min.) were determined by integration of the signal using the integrator C-R5A. Figure 2 depicts a typical chromatogram of PO in the atmosphere of the animal exposure chamber.

Calibration of propylene oxide

Calibration curves were obtained by plotting PO concentrations against the corresponding mean peak area or mean peak height (Figure 3). For this purpose, various PO concentrations were adjusted by injecting definite volumes of liquid PO into a desiccator using Hamilton syringes. The volume was calculated according to equation 1.

(1) $$V_{PO,De} = \frac{C_{PO,De} \times V_{De} \times MW_{PO}}{d_{PO} \times V_m \times 10^3}$$

$V_{PO, De}$ Volume of liquid PO in the desiccator (µl)

$C_{PO, De}$ Target PO concentration in the desiccator (ppm)

V_{De} Volume of the desiccator (ml)

MW_{PO} Molecular weight of PO: 58.1 g/mol

d_{PO} Density of PO: 0.830 g/ml (20°C)

V_m Molar gas volume of an ideal gas at 25°C and an atmospheric pressure of 720 torr: 25826 ml/mol

Homogeneous atmosphere in the desiccator containing PO was achieved using a magnetic stirrer. Gas samples were withdrawn from the desiccator through the teflon coated rubber septum using Hamilton syringes and were injected directly into the GC column.

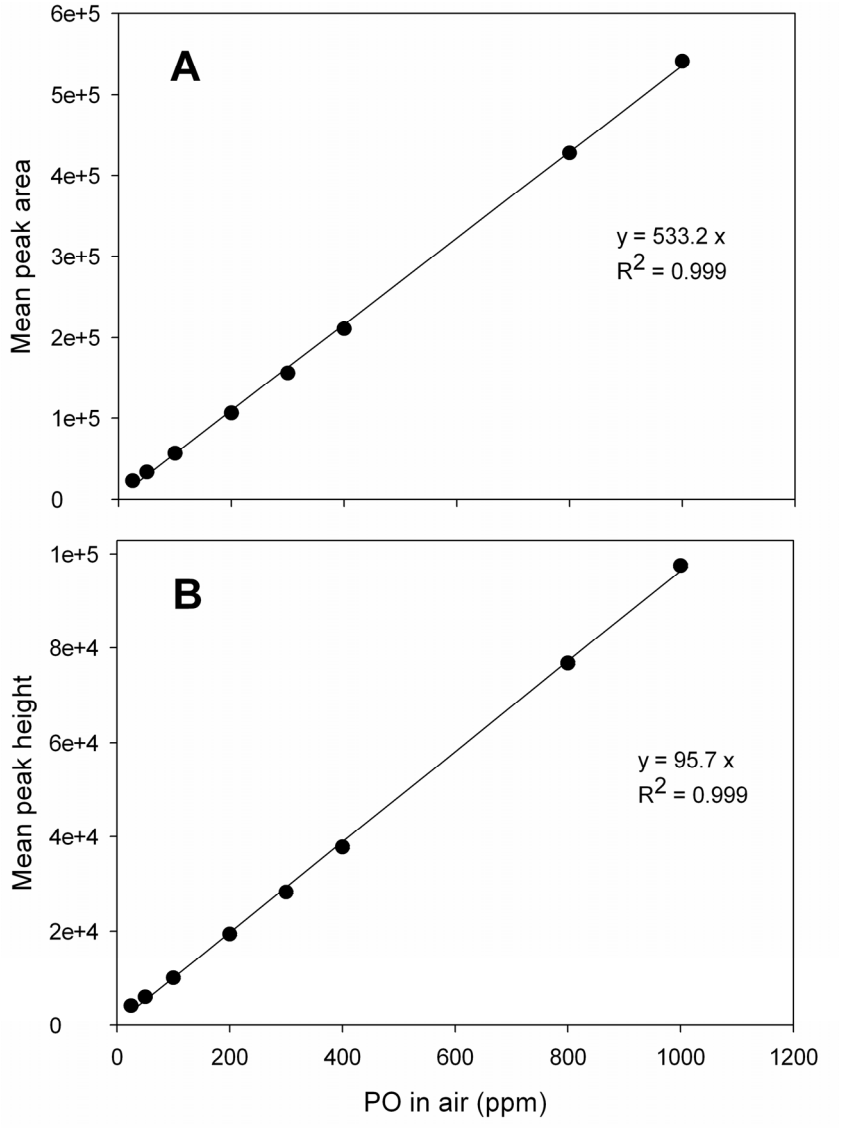

Figure 3: Calibration graphs for the determination of propylene oxide (PO). (A) PO concentration in air vs. mean peak area. (B) PO concentration in air vs. mean peak height.

To verify proportionality between detector signal and PO concentration, calibration samples with concentrations of 25–1000 ppm PO were prepared. Calibration samples were analyzed in triplicates. The calibration curves obtained by linear regression analysis through the origin showed correlation coefficients of 0.999 (Figure 3). The limit of detection, defined as a signal-to-noise ratio of 3, was not investigated since PO concentrations were considerably above the limit. Before starting the PO exposure on each day, a one-point calibration was carried out using a desiccator containing the desired PO concentration. The concentration was analyzed three times and the mean value was calculated.

2.3.2 Administration of bromodeoxyuridine through osmotic pumps

Osmotic mini pumps containing a sterile solution of 5-bromodeoxyuridine (BrdU; 20 mg/ml in saline) were implanted sc into the animals one day prior to PO exposure or treatment with DEM or BSO. As a thymidine analog, BrdU is incorporated into DNA during the S-phase of the cell cycle. Before implantation, the pumps were incubated in saline for 1-2 h at room temperature in order to ensure immediate function. Animals were anaesthetized in a closed desiccator using isoflurane at a concentration of 2% in air. After ensuring anesthesia, the skin covering the thoracolumbar area was shaved. During the surgery, anesthesia was maintained by constant supplying isoflurane via a tube attached to the nose of the animal. The shaved skin was cut transversely and extended longitudinally in the direction of the head. Then, the osmotic mini pump was inserted so that the flow moderator of the pump was directed to the head of the animal. The wound was closed with surgical clips. Rats were

observed until they were fully awake. Each rat was housed separately following insertion of the osmotic pumps.

2.3.3 Exposure to propylene oxide

Animals were exposed to constant atmospheric PO concentrations of 50, 100, 200, or 300 ppm for up to 3 days and for up to 6 h/day under atmospheric pressure and room temperature.

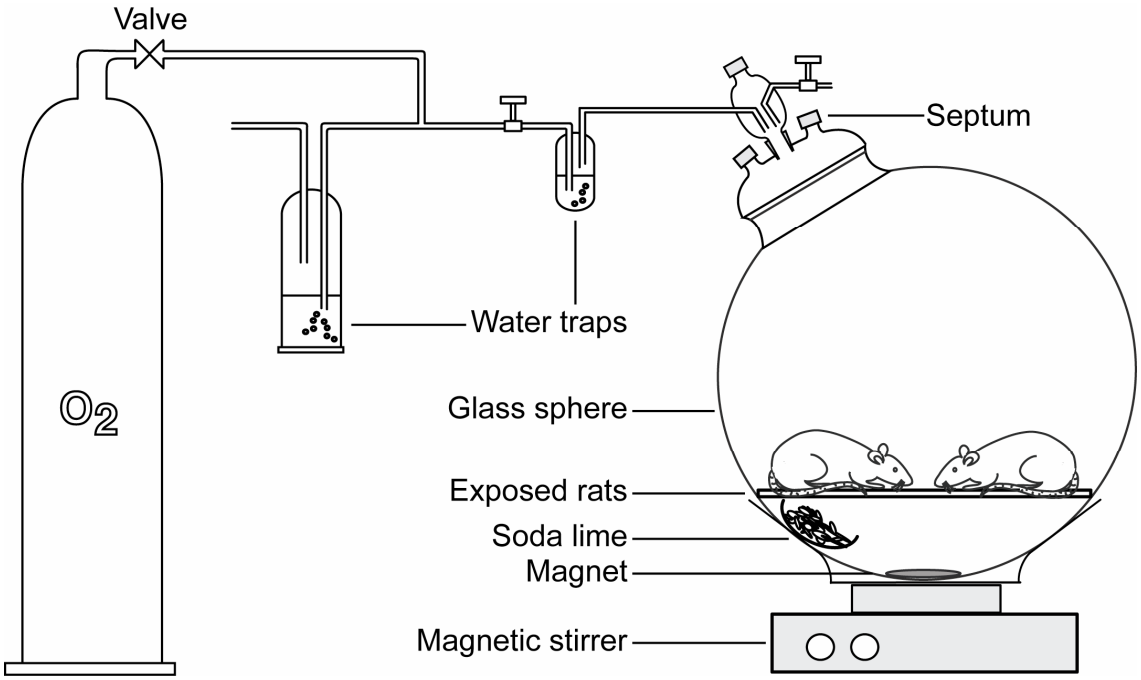

Figure 4: All glass system for exposing laboratory animals (Filser, 1992).

The number (n) of individual exposures were: n=15 (50 ppm PO), n=12 (100 ppm PO), n=9 (200 ppm PO), and n=19 (300 ppm PO). For the 3-day exposure studies (6 h/d), numbers (n) of animals were: NPSH determination, n=14 (0 ppm PO), n=4 (50 ppm PO), n=7 (100 ppm PO), n=4 (200 ppm PO), n=6 (300 ppm PO); determination of cell proliferation, n=14 (0 ppm PO), n=6 (each PO exposure

concentration >0 ppm PO). The number (n) of animals used in order to study daily NPSH concentration-time courses at 50, 100, and 300 ppm PO were each: n=3 (day 1), n=4 (days 2 and 3).

The exposure system consisted of a glass-sphere (63 l), equipped with an 8 cm long neck (inner diameter 15 cm) closed by a round lid with three ports (Figure 4). Two ports were covered by Teflon-coated synthetic rubber septa, the third one was connected to a passive oxygen supply system. The sphere contained a circular, foldable floor plate of solvent-inert polyvinylidene fluoride with a diameter of 40 cm.

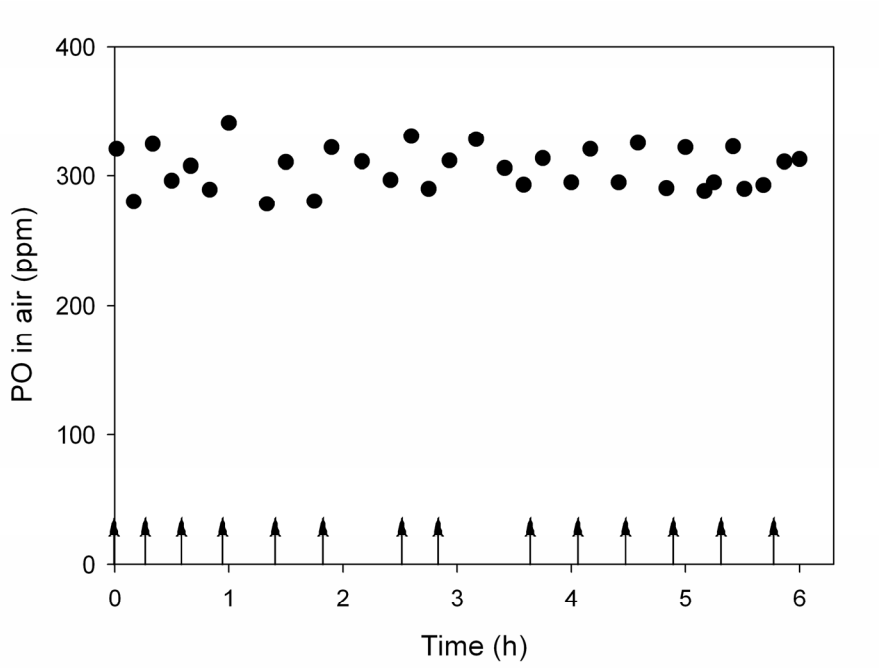

Figure 5: Typical concentration-time profile of propylene oxide (PO) in the atmosphere of the animal exposure chamber (63 l) during a 6 h exposure of 4 animals to 300 ppm.
Arrows represent the time points of re-injections of PO into the chamber atmosphere.

Exhaled CO_2 was trapped with 80 g soda lime placed below the floor plate. The concentration of PO in the chamber was determined by gas chromatography

and kept constant by injecting repeatedly liquid PO in order to compensate the loss of PO by metabolism.

In order to ensure a homogeneous atmosphere a magnetic stirrer was used. Figure 5 shows a typical concentration-time graph of PO measured in the atmosphere of the exposure chamber.

Time-weighted mean atmospheric exposure concentration was calculated by using the atmospheric concentrations determined at each time point successively during the given exposure period (Equation 2). The standard deviation (Equation 3) was calculated according to Sachs (1997).

(2) $$\overline{C}_{tw} = \frac{1}{T} \sum_{i=1}^{N-1} \left(\frac{C_i + C_{i+1}}{2} \right) * \left(t_{i+1} - t_i \right)$$

(3) $$SD_{tw} = \sqrt{\sum_{i=1}^{N-1} \left(\frac{C_i + C_{i+1}}{2} - \overline{C}_{tw} \right)^2 * \frac{t_{i+1} - t_i}{T}}$$

$\overline{C}_{tw}$	Time weighted mean PO concentration in the atmosphere
C_i	PO concentration at time point t_i
t_i	Time point of exposure
N	Number of measurements
T	Total exposure period
SD_{tw}	Standard deviation of the time weighted average concentration

The mean exposure concentrations varied not more than 6% from the target concentrations (comparison of mean values; Table 1).

Table 1: Target and actual exposure concentrations of propylene oxide (PO).

Target PO exposure concentration (ppm)	Actual PO exposure concentration (ppm) mean ± SD (n)*
50	51.6 ± 1.3 (15)
100	106.0 ± 4.0 (12)
200	206.0 ± 2.5 (9)
300	307.9 ± 5.9 (19)

*Number of individual experiments (6 h exposure)

2.3.4 Treatment with diethylmaleate, L-buthionine sulfoximine, and N-acetylcysteine

DEM (1.0 M) in olive oil was administered by ip injections on three consecutive days using two treatment regiments: either 2x250 mg/kg/day (time intervals of 3.5 h between the two dosages), or 500+150 mg/kg/day on days one and two (time intervals of 6 h between the two dosages) and a single dose of 500 mg/kg on day three. In the following, the two DEM treatment groups are named "2x250 mg/kg/day DEM" and "500+150 mg/kg/day DEM". BSO (0.45 M solution in saline) was administered ip at a single dose of 500 mg/kg/day on 3 consecutive days. NAC treatment was performed with animals exposed to 300 ppm PO for three days (6 h/day). NAC was given by sc injections on the three consecutive days with a total daily dose of 1,000 mg/kg (two daily treatments

with 500 mg/kg each with a time interval of 2.5 h between the dosages; first daily treatment 30 min before starting PO exposure).

Number (n) of animals used for the daily treatments with 2x250 mg/kg/day DEM over 3 days were: NPSH determination, n=3; determination of cell proliferation, n=6. The number (n) of animals used in order to study daily NPSH concentration-time courses were: n=3 (days 1 and 3), n=4 (day 2). Number (n) of animals used for the daily treatments with 500+150 mg/kg/day DEM over 3 days were: NPSH determination, n=3; determination of cell proliferation, n=4. The number (n) of animals used in order to study daily NPSH concentration-time courses were: n=3 (days 1 and 3), n=4 (day 2). Number (n) of animals used for the daily treatments with BSO over 3 days were: NPSH determination, n=5; determination of cell proliferation, n=6. The number (n) of animals used in order to study daily NPSH concentration-time courses were: n=8 (day 1), n=4 (day 2), and n=3 (day 3). Number (n) of animals used for the daily treatments with NAC in combination with PO exposure over 3 days were: NPSH determination, n=5; determination of cell proliferation, n=3. Nine animals were used in order to study the NPSH concentration-time course on day one.

2.3.5 Tissue preparation for the determination of non-protein thiol

In the PO exposure studies, animals were sacrificed immediately at the end of exposure. Animals treated with DEM or BSO were sacrificed at selected time points. When receiving either 2x250 mg/kg/day DEM or BSO for three consecutive days, rats were sacrificed 6 h after the first injection on day three. Rats administered 500+150 mg/kg/day DEM were sacrificed 7 h after treatment on the third day. All animals were euthanized by means of CO_2 asphyxiation.

RNE was isolated as described previously (Casanova-Schmitz et al., 1984). Briefly, the rat was decapitated, mandible, skin and eyes were removed, and the nasal cavity was opened sagittally. The isolation of RNE was performed under the stereomicroscope Stemi SV11. The RNE was collected from the naso- and maxilloturbinates, lateral walls, and septum anterior to the olfactory epithelium. The pooled RNE samples were placed into Eppendorf cups of 2.0 ml containing 0.9 ml of an ice-cold ammonium acetate buffer (5 mmol/l, pH 7.0). After shock freezing in liquid nitrogen, the cups were stored at -80°C. The total amount of RNE was 25-30 mg per animal.

2.3.6 Determination of non-protein thiol in respiratory nasal tissue

The concentration of NPSH was determined according to Lee et al. (2005) using Ellman's reagent. The frozen RNE containing ammonium acetate buffer was thawed on ice and RNE was homogenized in an ice-cooled 2-ml Teflon-glass homogenizer. An aliquot of 0.3 ml of the homogenate was mixed with 0.7 ml protein precipitation solution (1.67% meta-phosphoric acid, 0.02% disodium ethylenediaminetetraacetate dihydrate, 30% NaCl in distilled water) and centrifuged at 16000 x g (5 min, 0°C, Sigma 4K10). The pH of the supernatant (0.5 ml) was adjusted to 6.0 using 60 µl of 1.0 mol/l NaOH. After adding 0.5 ml of 1.0 mmol/l 5,5'-dithiobis-(2-nitrobenzoic acid) in 1% trisodium citrate dihydrate, the mixture was incubated in the dark at room temperature for 15 min. Thereafter, the extinction was measured at 412 nm against the respective blank samples. The blank samples were prepared by the same procedure as the tissue samples with the exception of adding ammonium acetate buffer instead of tissue homogenate. Calibration samples were prepared in ammonium acetate buffer by adding GSH at final concentrations of 0.005-0.3 mmol/l; this

concentration range resulted in linear calibration curves (Figure 6). Measurements were carried out in duplicates and mean values were used for the calculations of NPSH concentrations. The NPSH concentration in the tissue was determined according to equation 4.

(4) $$C_{NPSH,tissue} = \frac{1}{a} \times \Delta E_{NPSH} \times F$$

$C_{NPSH,tissue}$ NPSH concentration in the tissue sample (µmol/g)

a Slope of the standard straight line (l/mmol)

ΔE_{NPSH} Extinction of the homogenate minus blank

F Dilution factor

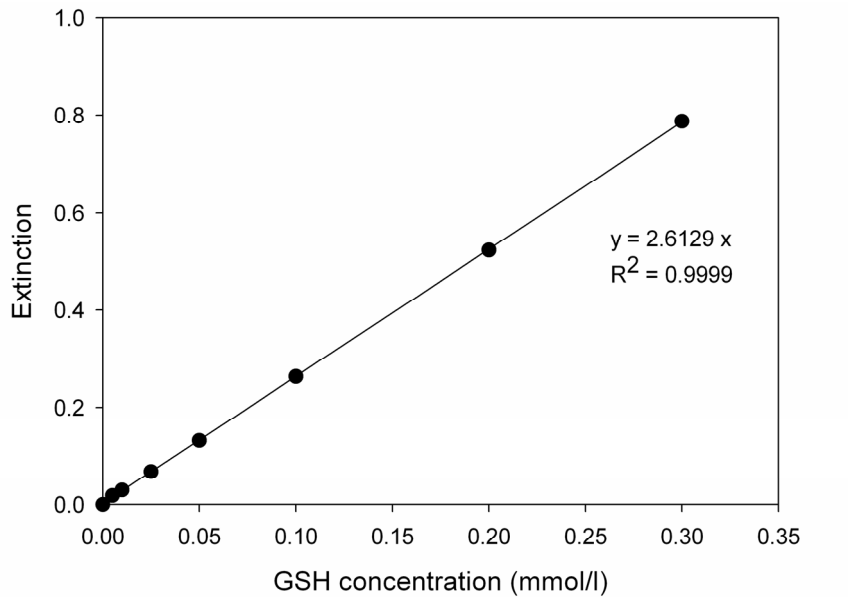

Figure 6: Calibration curve for the determination of NPSH. Extinction was measured at 412 nm.

2.3.7 Tissue preparation for histopathology and immunohistochemistry

On the third exposure day, animals were sacrificed: those treated with 500+150 mg/kg/day DEM after 5 h, those treated with 2x250 mg/kg/day DEM or BSO 6 h after the first injection, and those exposed to PO immediately following the 6-h exposures. After CO_2 asphyxiation and decapitation, eyes, lower jaw, skin, and musculature were removed. The skull was fixed in 4% neutral buffered formalin for 4 days at room temperature. Thereafter, tissue sections (2-3 mm) were cut cross-sectionally, placed in tissue cassettes and incubated in freshly prepared formalin for 3 days. For decalcification, the cassettes were rinsed with tap water for 30 min and transferred into 0.53 mol/l ethylenediaminetetraacetic acid (pH 7.4) for two weeks at 50°C. Then, the cassettes were placed in the vacuum infiltration processor Tissue-Tek® for 19.5 h at 58°C in order to remove water from the tissue sections.

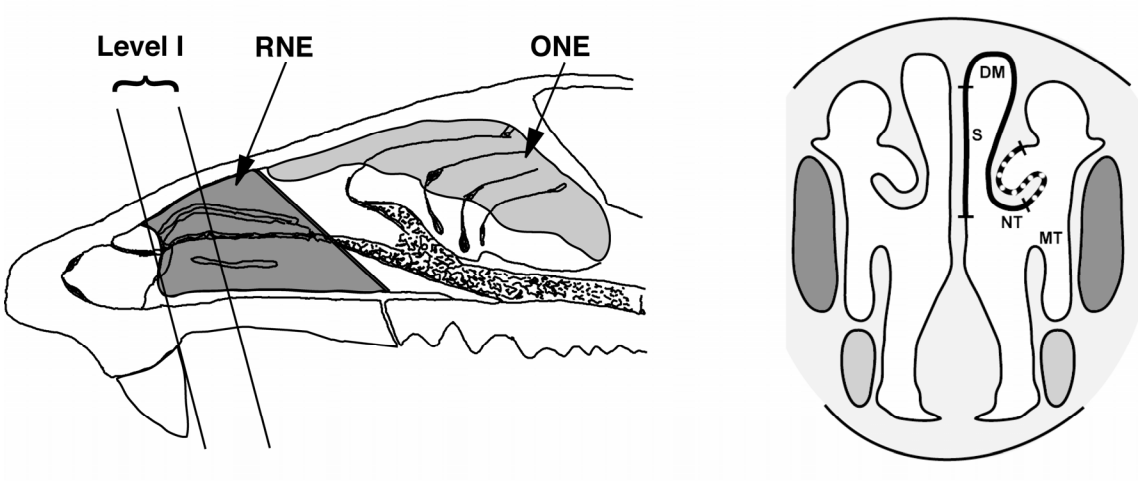

Figure 7: Lateral view of the rat nose (left) and cross section of level I (right). RNE: respiratory nasal epithelium; ONE: olfactory nasal epithelium; S: septum; DM: dorsal medial meatus; NT: nasoturbinate; MT: maxilloturbinate; solid bold line: mucociliary epithelium; dashed bold line: transitional epithelium.

After embedding the tissue sections into paraffin with the anterior face down, sections (for histopathology 3 μm and for immunostaining 1.5 μm thickness) from level I (Figure 7) were prepared for light microscopy (Zeiss microscope, AXIOPLAN) and evaluation of cell proliferation. Level I is located directly posterior to the upper incisor teeth and comprises the naso- and maxilloturbinates (Young, 1981) with the specific region where nasal tumors developed in F344 rats during the cancer bioassay (NTP, 1985; Ríos-Blanco et al., 2003b).

2.3.8 Histopathology

For histopathology examination tissue sections (3 μm) were cut from paraffin blocks and mounted on SuperFrost® slides. Slides were stored in an oven over night at 50°C and deparaffinized and stained with hematoxylin and eosin according to the following procedure.

(I) Slides were placed in a glass slide holder.

(II) Sections were deparaffinized and rehydrated by dipping the slide holder according to the following orders:

3 x 3 min in 100% xylene
3 x 3 min in 100% ethanol
1 x 3 min in 96% ethanol
1 x 3 min in 80% ethanol
1 x 3 min in 70% ethanol
1 x 3 min in 50% ethanol
1 x 3 min in 30% ethanol
1 x 5 min in deionized water

(III) Hematoxylin staining:

1 x 3 min in Hematoxylin (1% in distilled water)

1 x 10 min in running tap water

Excess water was removed from slide holder before the eosin staining.

(IV) Eosin staining and dehydration:

1 x 2 min in aqueous eosin (1% in distilled water)

3 x 5 min in 96% in ethanol

3 x 5 min in 100% in ethanol

3 x 15 min in 100% xylene

(V) The slides were immediately covered using Pertex® and dried overnight in the fume hood.

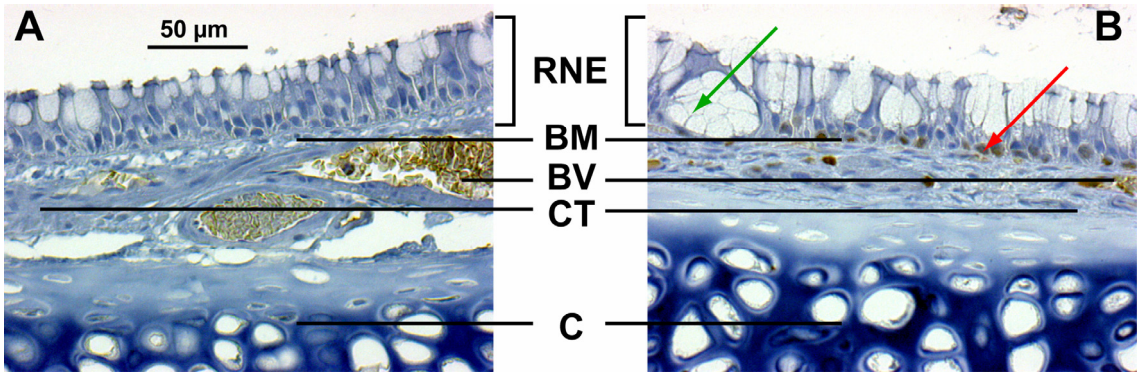

Figure 8: Photomicrographs of rat respiratory nasal epithelium (RNE) from the mucociliary epithelium of septum stained with BrdU antibody.
A: control animal; B: animal exposed to 300 ppm PO for 3 days. Red arrow: BrdU positive cell. Green arrow: mucous cell nest. BM: basement membrane; BV: blood vessel; CT: connective tissue; C: cartilage.

Level I of the rat nose was examined for the following lesions: edema, degeneration of respiratory epithelia, rhinitis, erosion of the turbinate

epithelium, squamous metaplasia, epithelial hyperplasia, mucous cell hypertrophy and hyperplasia, changes in mucous secretion, and apoptosis. Slides were evaluated blindly (Institute of Pathology, Helmholtz Zentrum München). The evaluation of mucous cell nests (Figure 8) was performed by counting the total number of cell nests in the nasal mucociliary epithelium lining the middle septum, the dorsal medial meatus, and the medial surface of the nasoturbinates as well as in the transitional epithelium lining the lateral surface of the nasoturbinate (Figure 7). One tissue section per animal was evaluated. Measurements were done on both side of the nasal cavity.

2.3.9 Bromodeoxyuridine immunostaining

For the determination of cell proliferation, the incorporation of BrdU into DNA was used. BrdU labeling was detected by immunohistochemistry. The basic principle of the procedure is illustrated in Figure 9. The tissue sections were deparaffinized and rehydrated to reduce background staining by non specific binding of antibodies to the paraffin. For this purpose, the slide holder containing tissue sections (1.5 μm) were dipped into the solutions according to the following orders:

3 x 3 min in 100% xylene
3 x 3 min in 100% ethanol
1 x 3 min in 96% ethanol
1 x 3 min in 80% ethanol
1 x 3 min in 70% ethanol
1 x 3 min in 50% ethanol
1 x 3 min in 30% ethanol
1 x 5 min in deionized water

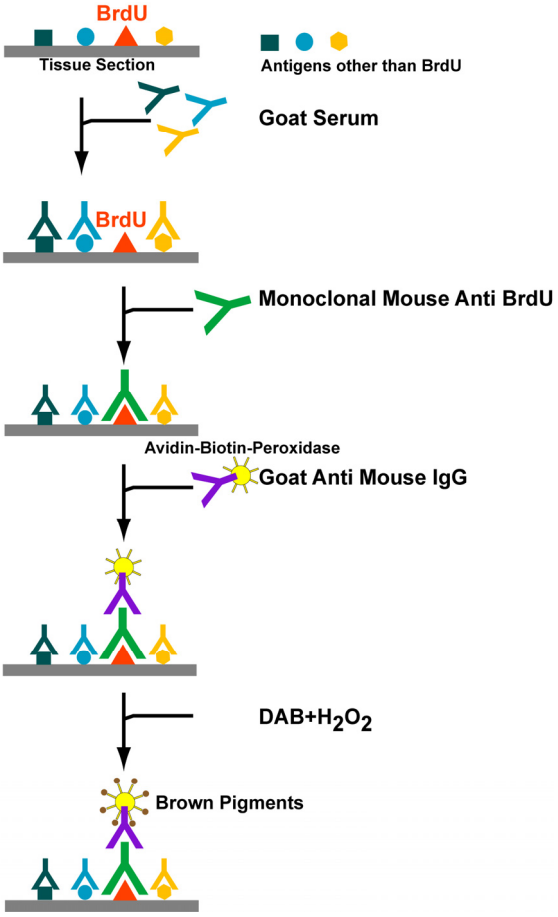

Figure 9: Scheme of the immunohistochemical procedure for detection of BrdU incorporation into DNA.
DAB: 3,3′-diaminobenzidine tetrahydrochloride; BrdU: bromodeoxyuridine

Then, the slides were placed in 0.01 mmol/l citrate buffer, pH 6.0, containing 0.1% Tween® 20 and heated in a microwave oven at 1000 W for 30 min to restore the three-dimensional structure of the BrdU epitopes which were masked during fixation process in the tissue preparation. Sections were washed in Tris-buffered saline (pH 7.6) containing 3% goat serum for 20-120 min in order to cover antigens other than BrdU. Thereafter, the monoclonal mouse anti-BrdU antibody (1:200 dilution with the diluent buffer of the iVIEW™ DAB Detection kit) was added, and the sections were kept in a wet chamber overnight at room temperature. The remaining procedure was performed in the

automated immunostainer (NexEs® IHC) using the detection kit iVIEW™ DAB detection kit according to the manufacturer's instruction. The goat anti-mouse IgG which is directed against the monoclonal mouse anti-BrdU antibody, was conjugated with a complex consisting of Avidin, Biotin, and a peroxidase. In presence of hydrogen peroxide, the peroxidase converts 3,3´-diaminobenzidine into an insoluble brown reaction product.

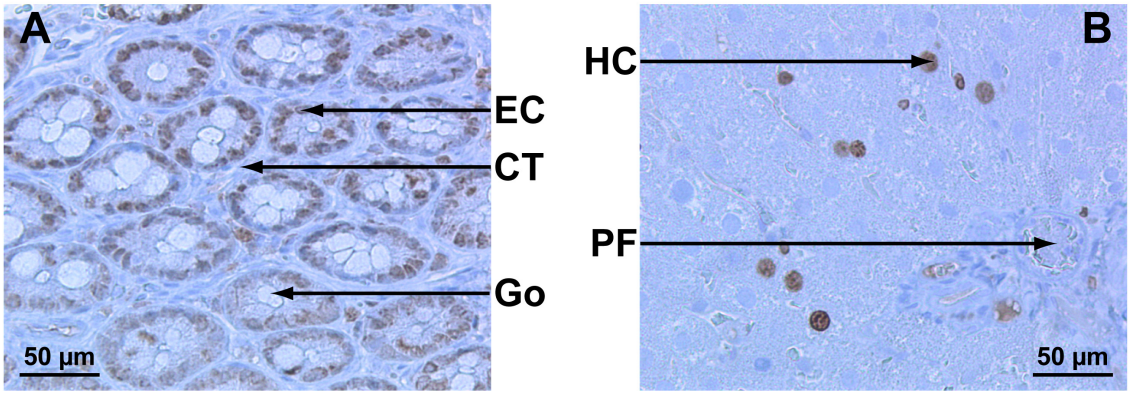

Figure 10: Photomicrographs of duodenum (A) and liver (B) of a control animal stained with BrdU antibody.
Brown pigmentations: S-phase positive cells.
EC: epithelial cell; CT: connective tissue; Go: goblet cell; HC: hepatocyte; PF: periportal triad consisting of bile duct, lymph vessel and hepatic artery.

Using the light microscope, BrdU positive cells could be recognized by this brown pigmentation of the nuclei after counterstaining with hematoxylin (Figure 8). The systemic delivery of BrdU was verified by positive staining of sections from the duodenum and from the liver of each animal (Figure 10).

2.3.10 Evaluation of bromodeoxyuridine incorporation

BrdU incorporation was examined (Figure 11) in the nasal mucociliary epithelium lining the region that comprises the middle septum, the dorsal

medial meatus and the medial surface of the nasoturbinates as well as in the transitional epithelium lining the lateral surface of the nasoturbinate (Figure 7).

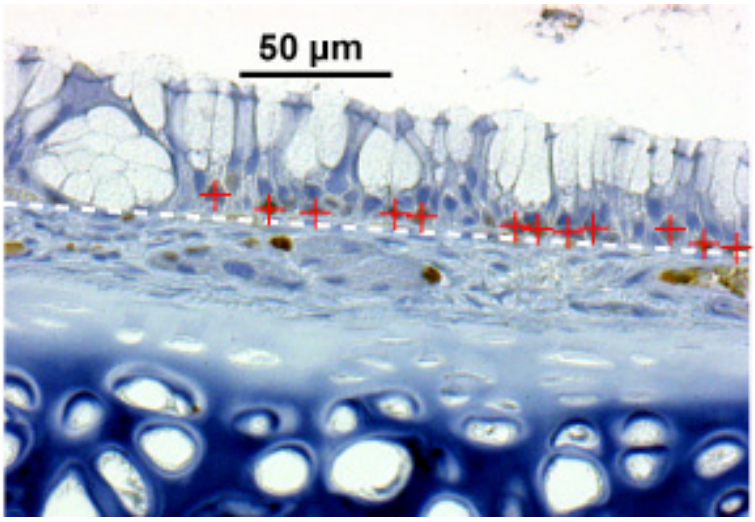

Figure 11: Determination of the Unit length Labeling index (ULLI) in rat respiratory nasal mucosa by using the Optimas image analysis software.
The ULLI was calculated by counting the number of BrdU positive cells (red crosses) per mm of basement membrane (white dashed line).

These epithelia include the specific anatomical regions where tumors had developed in the cancer bioassay of NTP (1985). According to NTP (1985) and a re-evaluation by Ríos-Blanco et al. (2003b) the tumors had developed in level I of RNE at the margin of the transitional epithelium in the ventral lateral surface of the nasoturbinate.

2.3.11 Statistical analysis

Unless otherwise noted, statistical analyses were done using one-way ANOVA followed by Tukey's multiple comparison post hoc test. For the evaluation of mucous cell nests, a non-parametric test (Kruskal-Wallis test) was used. The level of statistical significance was set at $p<0.05$.

3 RESULTS

3.1 Body weight development and histopathological findings

Body weights of most of the rats were recorded once a day during the 3-days of exposure to PO, PO plus NAC, or treatment with DEM or BSO (Table 2). In addition, the animals were observed for overt signs of toxicity. A Statistically significant decrease in body weight was observed only in animals exposed to 300 ppm PO and co-treated with NAC. This could be interpreted as a hint of acute toxicity.

Table 2: Body weight development of the rats exposed to propylene oxide (PO), PO plus N-acetylcysteine (NAC) or treated with diethylmaleate (DEM) or buthionine sulfoximine (BSO).

Animal group (n: number of animals)	Body weight (g) (mean±SD)		Realative individual body weight after 3 days (%)*
	Day 1	Day 3	(mean±SD)
Control (n=13)	247±11.5	248±11.0	100.4±1.8
Control (olive oil) (n=3)	221±15.0	214±18.6	96.8±2.2
50 ppm PO (n=12)	239±4.3	239±6.5	100.4±1.6
100 ppm PO (n=13)	248±15.1	248±15.0	100.0±1.9
200 ppm PO (n=10)	227±30.9	232±19.9	103.2±6.7
300 ppm PO (n=8)	234±12.8	230±13.9	98.3±1.3
NAC+300 ppm PO (n=5)	251±4.1	237±8.7[#]	94.5±3.1[+]
2x250 mg/kg/day DEM (olive oil; n=7)	241±10.2	233±9.0	97.0±1.5[a]
500+150 mg/kg/day DEM (olive oil; n=9)	232±19.6	216±17.9	93.0±2.1[a]
500 mg/kg/day BSO (n=7)	250±5.8	246±7.9	98.3±1.7

*: Body weight of each individual rat was set to 100% on day one before start of exposure. #: Statistically significantly different as compared to body weight on day one (t-test). +: Statistically significantly different concerning relative body weight changes between controls and exposed animals (ANOVA). a: ANOVA was carried by comparing with vehicle controls (olive oil).

For histopathology, tissue sections from level I of the nose (see Figure 7) were examined. This level comprises the specific region where nasal tumors developed in F344 rats. The nasal passage of rats at level I is characterized by three types of respiratory epithelia (Boorman et al., 1990): The ventral surface is lined by a stratified squamous epithelium. The RNE lining the septum, dorsal medial meatus, and medial surface of the nasoturbinate (see Figure 7)

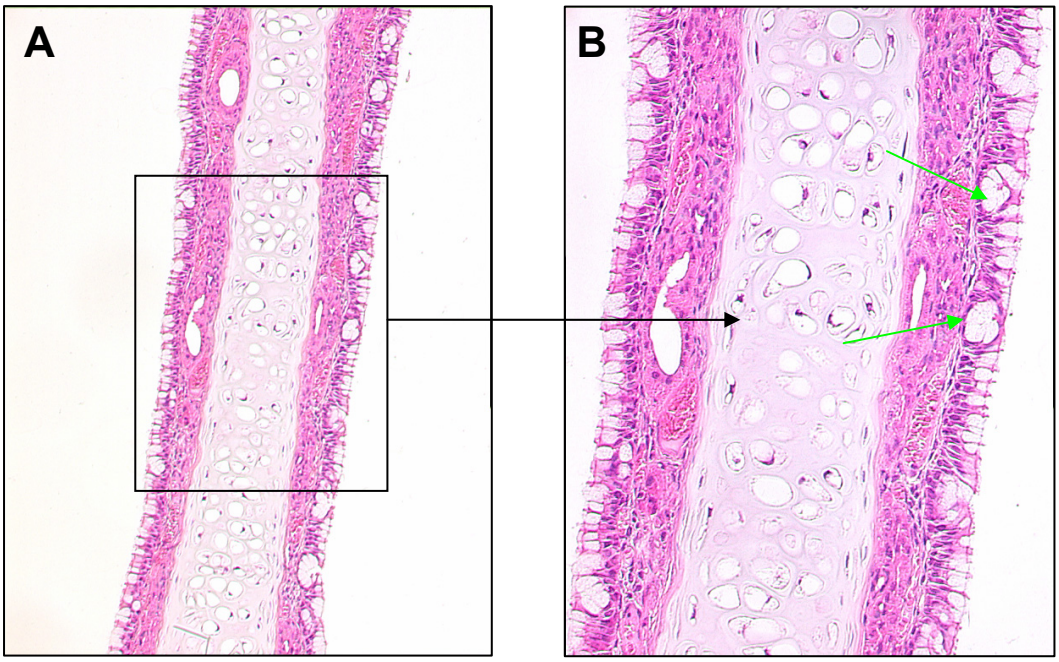

Figure 12: Hematoxylin and eosin staining of the respiratory nasal epithelium (septum) of rats exposed to 300 ppm PO for 3 days.
(A) Original magnification x25. (B) Original magnification x100. Green arrows: mucous cell nests.

is composed of highly ciliated and nonciliated columnar cells, mucous cells, brush cells, and basal cells. The basal cells differentiate into the distinctive mature cells of epithelium. The epithelium lining the lateral surface of the nasoturbinate is nonciliated or sparsely ciliated and it is composed of cuboidal cells. In the present study, the RNE lining the septum, dorsal medial meatus, and medial surface of the nasoturbinate is referred to as mucociliary epithelium

and the epithelium lining the lateral part of the nasoturbinate is referred to as transitional epithelium. Histopathological examination of RNE (level I) did not

Table 3: Total number of mucous cell nests lining the medial septum, dorsal medial meatus and medial surface of the nasoturbinates in both sides of nasal cavities (level I) of rats exposed to propylene oxide (PO) or PO plus N-acetylcysteine (NAC) or treated with diethylmaleate (DEM) or buthionine sulfoximine (BSO) for 3 days.*

Animal group (n: number of animals)	Number of mucous cell nests (mean±SD)
Control (n=14)	6.0±2.7
50 ppm PO (n=6)	6.5±5.2
100 ppm PO (n=6)	5.3±2.0
200 ppm PO (n=6)	6.7±4.5
300 ppm PO (n=6)	7.0±2.4
NAC+300 ppm PO (n=3)	6.3±4.3
2x250 mg/kg/day DEM (n=6)	6.2±4.3
500+150 mg/kg/day DEM (n=4)	7.5±1.7
500 mg/kg/day BSO (n=6)	5.5±2.6

*: The tissue sections examined were identical to those used for the quantification of cell proliferation.

reveal any exposure- or treatment-related effect in either the mucociliary epithelium or in the transitional epithelium. Special attention was given on the mucous cell nests, which had been previously shown to be a specific lesion upon 4 weeks of PO exposure (Ríos-Blanco et al., 2003b). In the present study, mucous cell nests (Figures 8, 12) were detected occasionally in both control and treatment groups but they were not significantly increased in number in any of the treatment or exposure groups after 3 days of exposure (Table 3). The numbers of animals per group given in Table 3 represent only a part of all animals used. The other animals were served for the determination the NPSH status in RNE.

3.2 Non-protein thiol status and cell proliferation in respiratory nasal epithelium

3.2.1 Exposure to propylene oxide

Figure 13 shows NPSH contents and cell proliferation in total investigated RNE of rats after inhalation exposure to 0, 50, 100, 200, or 300 ppm PO for 3 days (6 h/day). In control rats, the average NPSH content in RNE was 4.7±0.8 μmol/g (mean±SD). Exposure to 50 ppm PO resulted in partial NPSH depletion of approximately 50% of the mean control value. At concentrations of 100 ppm and above, NPSH level was minimum at 24-28% (~1.25 μmol/g w.w.) of the mean NPSH content in controls (Figure 13). Cell proliferation in total RNE of PO exposed rats, expressed as ULLI, is also illustrated in Figure 13. In control rats, 5.0±2.1 S-phase positive cells were detected per mm of basement membrane lining the septum, dorsal medial meatus, and the lateral-ventral part of the nasoturbinates. At 50 ppm PO, the ULLI was similar to that of control

animals. At 100 ppm PO, a 2.0-fold statistically significant increase in cell proliferation over the control was observed.

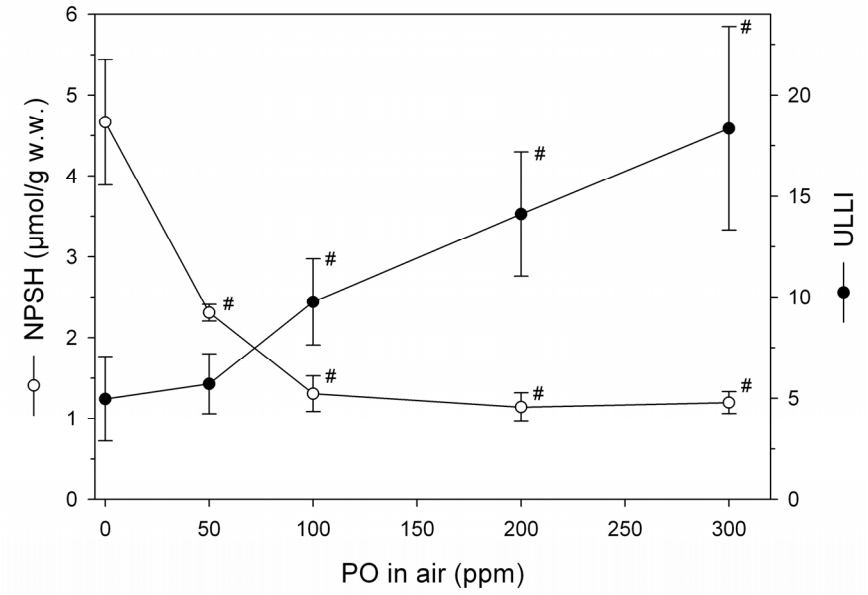

Figure 13: Non-protein thiol (NPSH) levels and cell proliferation in rat nasal respiratory epithelium lining the septum, dorsal medial meatus, and lateral-ventral surface of the nasoturbinate after exposure (6 h/day, 3 days) to propylene oxide (PO). Proliferation data are given as Unit Length Labeling Index (ULLI). Data represent means and standard deviations. Numbers (n) of animals were: NPSH, n=14 (0 ppm PO), n=4 (50 ppm PO), n=7 (100 ppm PO), n=4 (200 ppm PO), n=6 (300 ppm PO); ULLI, n=14 (0 ppm PO), n=6 (each PO exposure concentration >0 ppm PO).
#: Statistically significantly different from controls.

Above 100 ppm PO, cell proliferation increased linearly with the PO exposure concentration up to 3.7-fold over the control value at 300 ppm PO.

Time dependent changes of NPSH contents in RNE are shown in Figure 14. Independently of the PO concentration, NPSH declined rapidly after starting the exposure on each day. In rats exposed to 50 ppm PO, except at day 1, NPSH levels in RNE never dropped below 2.2 µmol/g at any of the time points investigated.

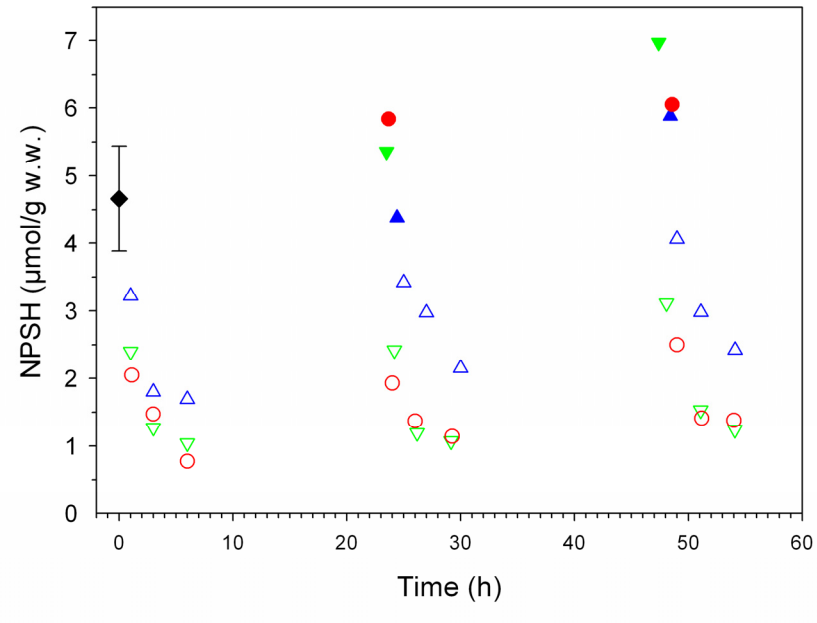

Figure 14: Time-dependent changes of non-protein thiol (NPSH) levels in respiratory nasal epithelium of rats during exposure to propylene oxide (PO). Filled diamond (black): controls (0 ppm PO); triangles up (blue): 50 ppm PO; triangles down (green): 100 ppm PO; circles (red): 300 ppm PO. Filled triangles and circles represent values obtained at beginning of the exposures on days 2 and 3. Symbol for the control value represents mean and standard deviation (n=14); symbols for PO exposed rats represent single values from individual animals.

In RNE of rats exposed to 100 and 300 ppm PO, NPSH contents reached the minimum value of approximately 1.25 µmol/g after 2-3 h after starting the exposure. At the beginning of the exposures on days 2 and 3, NPSH contents were completely replenished and, with the exception of the animal exposed to 50 ppm on the second day, even exceeded the NPSH concentration in RNE of controls up to 148% (100 ppm, day 3).

Figure 15 shows the occurrence of cell proliferation in discrete RNE regions (see Figure 7) of controls and rats exposed to PO for 3 days (6 h/day). In controls and in animals exposed to 50 ppm PO, none of the RNE regions showed a significant increase in S-phase positive cells. In rats exposed to 100 ppm PO, a

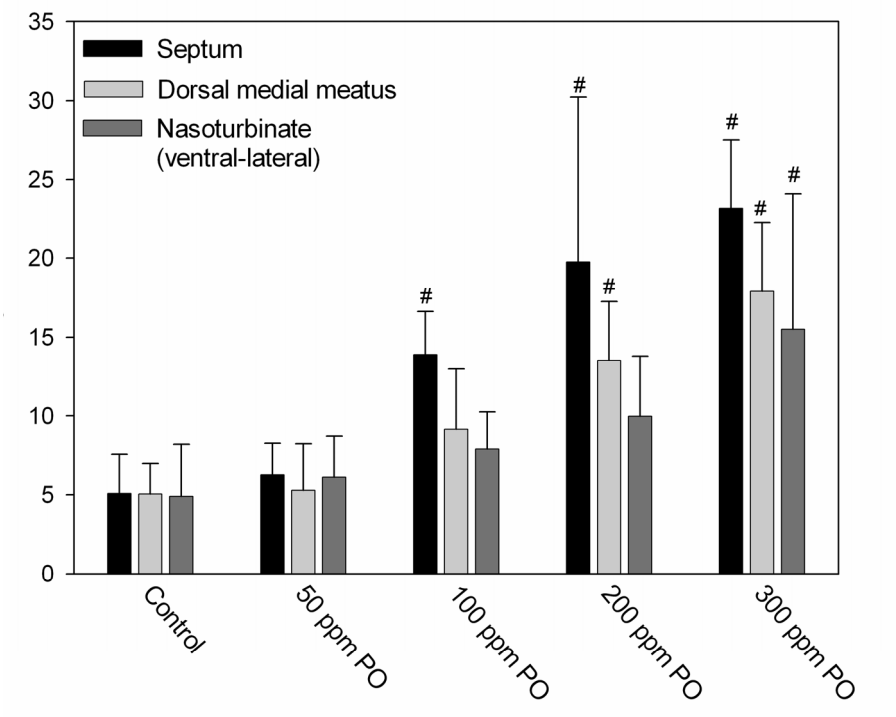

Figure 15: Cell proliferation in discrete regions of rat respiratory nasal epithelium after 3 days of exposure (6 h/day) to propylene oxide (PO).
Details on exposures and treatments are given in the Materials and Methods section. Proliferation data are given as Unit Length Labeling Index (ULLI). Data represent means and standard deviations (controls: n=14; PO exposure groups: n=6). #: Statistically significantly different from controls.

statistically significant increase in cell proliferation was only noted in the epithelium lining the septum. At 200 ppm PO, the number of S-phase positive cells was increased in the mucociliary epithelium of both the septum and the dorsal medial meatus but not in the transitional epithelium of the nasoturbinates. After exposure to 300 ppm PO, cell proliferation was increased in all RNE regions.

3.2.2 Effect of N-acetylcysteine on propylene oxide exposure

In RNE of rats exposed to 300 ppm PO (6 h/day, 3 days) and treated simultaneously with NAC, the NPSH content of 2.5±0.6 µmol/g wet weight (mean±SD), was significantly lower than that in controls, but significantly higher than that of rats exposed solely to 300 ppm PO. Time dependent changes of NPSH contents in RNE of rats exposed to 300 ppm PO and simultaneously treated with NAC were investigated on the first day of exposure (6 h; Figure 17).

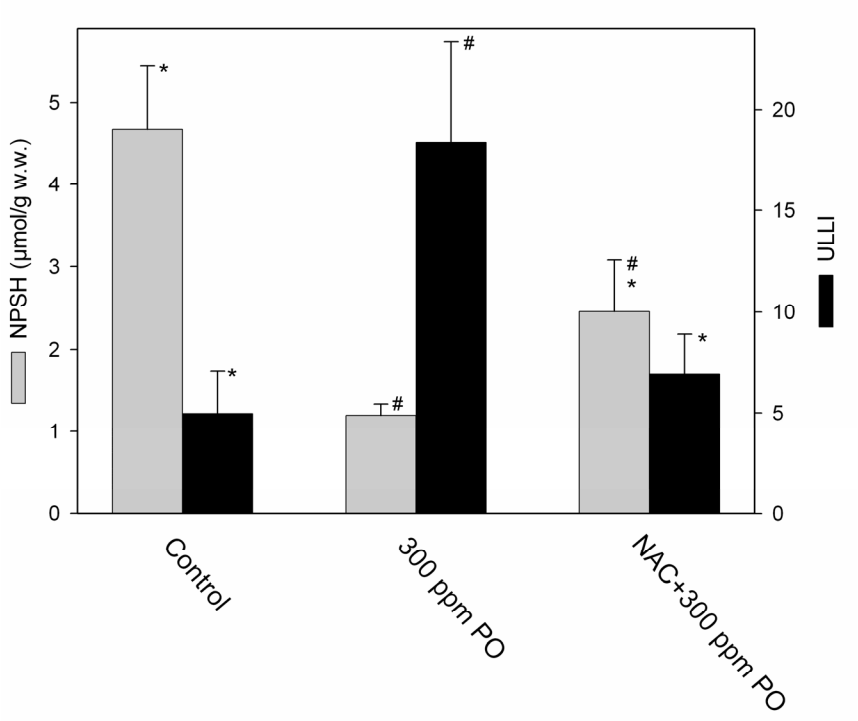

Figure 16: Non-protein thiol (NPSH) levels and cell proliferation in respiratory nasal epithelium of rats exposed to 300 ppm propylene oxide (PO; 6 h/day, 3 days) with and without co-treatment with N-acetylcysteine (NAC).
Details on the NAC treatment are given in the Materials and Methods section. Proliferation data are given as Unit Length Labeling Index (ULLI). Data represent means and standard deviations. Number (n) of animals were: NPSH, n=14 (controls), n=6 (300 ppm PO), n=5 (NAC+300 ppm PO); ULLI, n=14 (controls), n=6 (300 ppm PO), n=3 (NAC+300 ppm PO). #: Statistically significantly different from controls. *: Statistically significantly different from animals solely exposed to 300 ppm PO.

In these rats, the NPSH content in RNE did not decline below 2.1 μmol/g wet weight. The findings agree with those observed after the end of the three-days exposures (Figure 16). Obviously, NAC treatment prevented the maximum NPSH depletion observed solely at 300 ppm PO on days one, two and three (Figures 14 and 16).

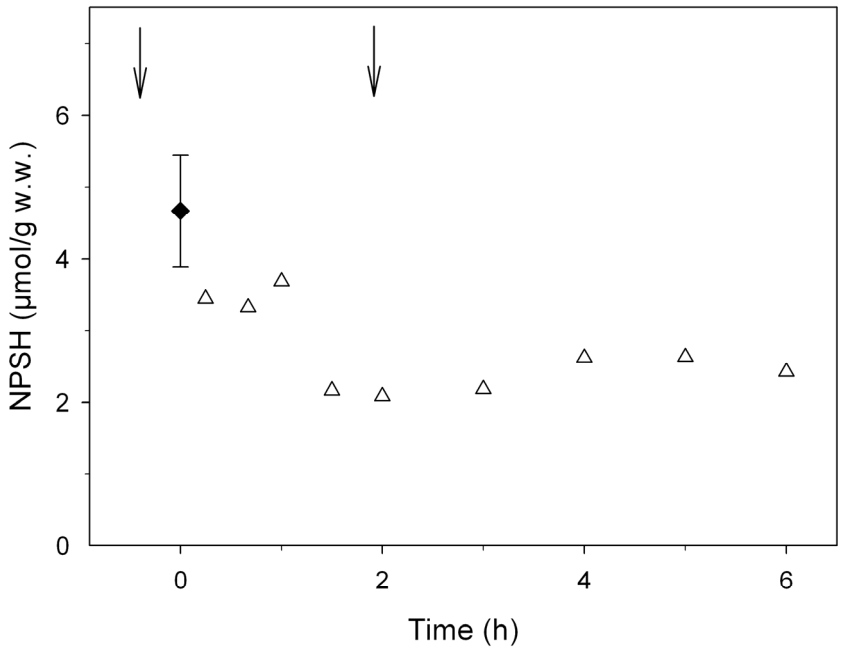

Figure 17: Time-dependent changes (day one of exposure) of non-protein thiol (NPSH) levels in respiratory nasal epithelium of rats exposed to 300 ppm propylene oxide (PO) and simultaneously treated with N-acetylcysteine (NAC). Details on the NAC treatment are given in the Materials and Methods section. Arrows indicate the time points of NAC administration. Symbol for the control value represents mean and standard deviation (n=14). Symbols for rats exposed to PO and simultaneously treated with NAC represent single values from individual animals.

Figure 18 shows the results on cell proliferation in discrete RNE regions (see Figure 7) of controls and rats exposed to 300 ppm PO with and without co-treatment with NAC. In contrast to RNE of rats exposed to 300 ppm PO only,

RNE of co-treated rats did not show a significant increase in S-phase positive cells in any of the regions investigated.

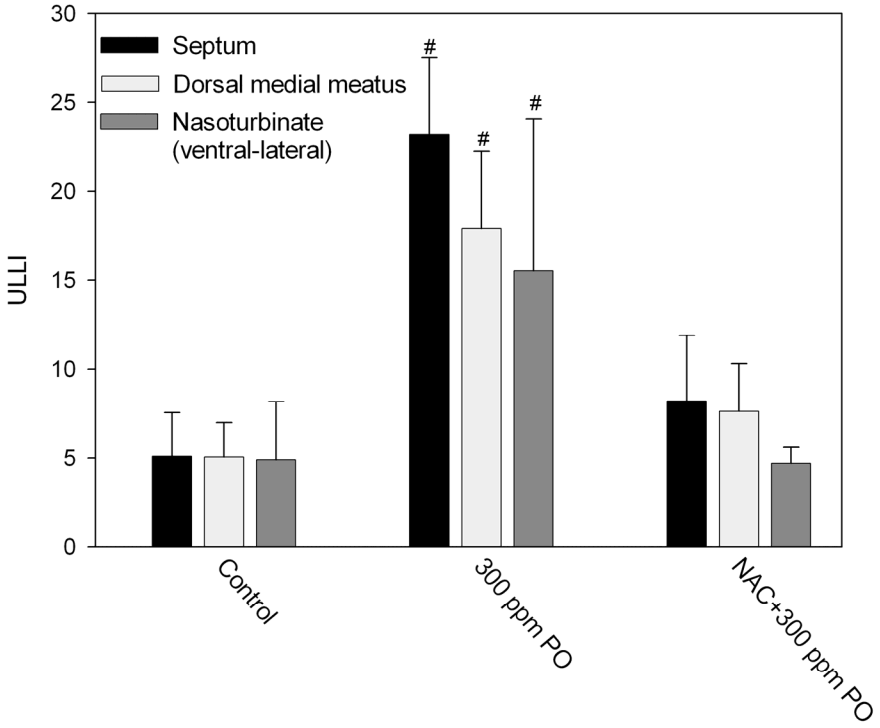

Figure 18: Cell proliferation in discrete regions of rat respiratory nasal epithelium after 3 days of exposure (6 h/day) to 300 ppm propylene oxide (PO) with and without co-treatment with N-acetylcysteine (NAC).
Details on the treatments are given in the Materials and Methods section. Proliferation data are given as Unit Length Labeling Index (ULLI). Data represent means and standard deviations (controls: n=14; 300 ppm PO: n=6; NAC+300 ppm PO: n=3). #: Statistically significantly different from controls.

3.2.3 Effects of diethylmaleate or L-buthionine sulfoximine on the non-protein thiol status in respiratory nasal epithelium

In rats treated with DEM, the effects on NPSH status and cell proliferation in RNE were dependent on the treatment regimen. Administration of 2x250 mg/kg/day DEM led to a statistically significantly reduced NPSH content in

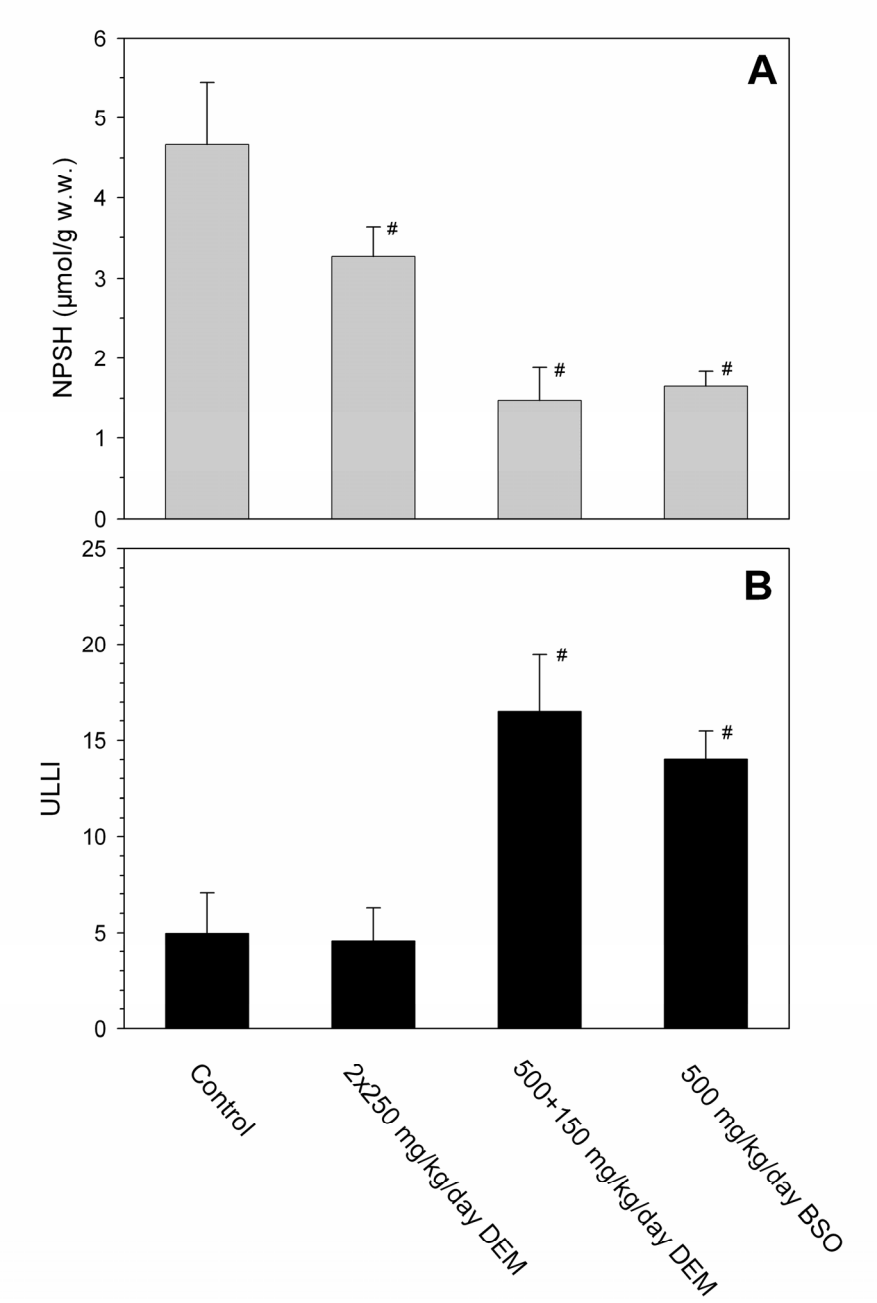

Figure 19: Non-protein thiol (NPSH) levels (A) and cell proliferation (B) in nasal respiratory epithelium of rats treated repeatedly with diethylmaleate (DEM) and buthionine sulfoximine (BSO) for 3 days.
Details on the treatments are given in the Materials and Methods section. Proliferation data are given as Unit Length Labeling Index (ULLI). Data represent means and standard deviations. Number (n) of animals were: NPSH, n=14 (controls), n=3 (DEM treatments), n=5 (BSO treatment); ULLI, n=4 (500+150 mg/kg/day DEM), n=6 (2x250 mg/kg/day DEM or 500 mg/kg/day BSO).
[#]: Statistically significantly different from controls.

RNE of 70% of that in control animals. No effect on cell proliferation was detected in these animals (Figure 19). Dosage of 500+150 mg/kg/day DEM resulted in NPSH depletion to about 32% of the control value, thus reaching approximately the minimum value observed in RNE of rats solely exposed to PO (≥100 ppm; Figure 13). Cell proliferation was significantly increased to 3.3-fold over controls (Figure 19). BSO treatment had a similar effect on RNE, as NPSH was almost at its minimum, and cell proliferation was significantly increased to 2.8-fold over controls (Figure 19).

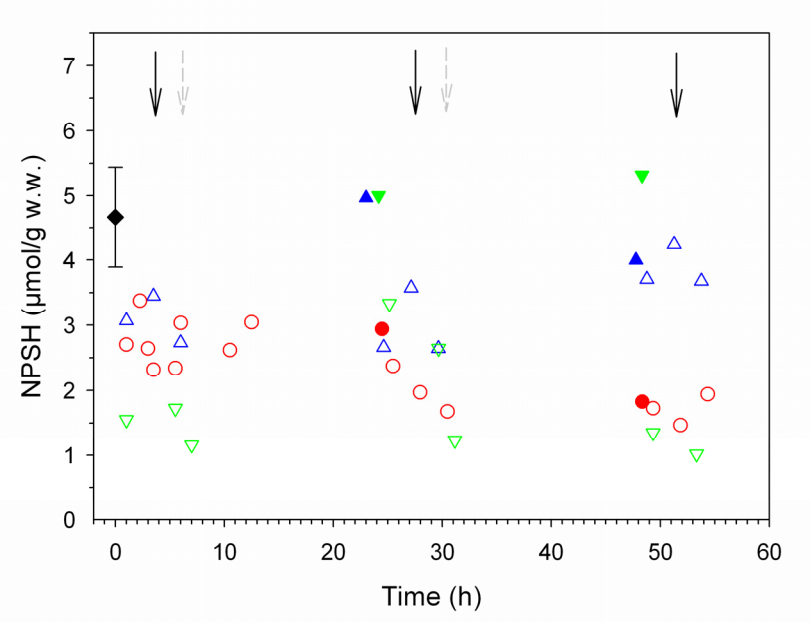

Figure 20: Time-dependent changes of non-protein thiol (NPSH) levels in respiratory nasal epithelium of rats during treatment with diethylmaleate (DEM) or buthionine sulfoximine (BSO).
Filled diamond (black): controls; triangles up (blue): 2x250 mg/kg/day DEM; triangles down (green): 500+150 mg/kg/day DEM; circles (red): 500 mg/kg/day BSO. Filled triangles and circles resemble data obtained when the animals received the first dose on days 2 and 3. Arrows indicate times of the second DEM dose (black solid: 250 mg/kg DEM; grey dashed: 150 mg/kg DEM). Symbol for the control value represents mean and standard deviation (n=14); symbols for DEM or BSO treated rats represent single values from individual animals.

Time dependent changes of NPSH contents in RNE of rats treated with DEM or BSO are shown in Figure 20. In DEM treated rats, there was a striking difference between the two treatment regimens: In RNE of rats given 2x250 mg DEM/kg/day, NPHS did not fall below a value of 2.6 μmol/g (about 56% of the control value) at any time point investigated.

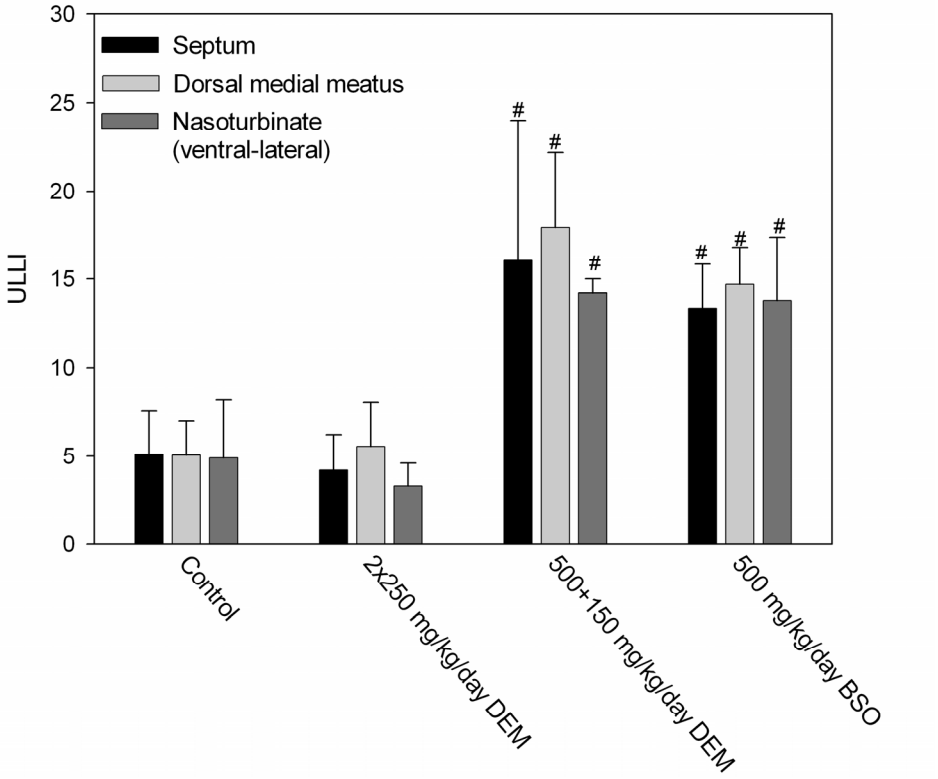

Figure 21: Cell proliferation in discrete regions of rat respiratory nasal epithelium after 3 days of repeated treatment with diethylmaleate (DEM) or buthionine sulfoximine (BSO).
Details on treatments are given in the Materials and Methods section. Proliferation data are given as Unit Length Labeling Index (ULLI). Data represent means and standard deviations (controls: n=14; 500+150 mg DEM/kg/day: n=4; 2x250 mg DEM/kg/day or 500 mg BSO/kg/day: n=6). #: Statistically significantly different from controls.

In contrast, treatment with 500+150 mg/kg/day DEM led to maximum NPSH depletion on each day. At both dosage regimens, NPSH was completely

replenished before the first treatment on days two and three and partially before the second daily dose. However, in contrast to the PO exposed animals, the NPSH level did not exceed the control value. BSO treatment showed different effects on the NPSH status on each day: On the first day, NPSH in RNE was only partially depleted to 50-72% of the control value. On the second day, BSO treatment resulted in a further, time dependent NPSH depletion almost to the minimum value. On the third day, the NPSH content was close to the minimum value at all time points investigated. No NPSH repletion at all could be detected after BSO treatment (Figure 20).

The occurrence of cell proliferation separately in different RNE regions (see Figure 7) of rats treated with DEM or BSO is shown in Figure 21. In animals treated with 2x250 mg/kg/day DEM, none of the RNE regions showed a significant increase in S-phase positive cells. After treatment with 500+150 mg/kg/day DEM or BSO, cell proliferation was significantly increased in all RNE regions investigated (Figure 21).

4 DISCUSSION

4.1 GSH depletion and cell proliferation in the respiratory nasal epithelium

The simultaneous occurrence of maximum NPSH depletion and cell proliferation in total RNE is in agreement with the assumption of Lee et al. (2005) that GSH homeostasis should play a pivotal role in controlling cell proliferation in RNE. The present study clearly demonstrated that cells in RNE proliferated only when NPSH was around its minimum, about 25% of the control value. According to Potter et al. (1995), the sum of GSH plus cystein — the latter formed from GSH during the surgical procedure — was 76% of the NPSH level in RNE of rats. Therefore, the residual NPSH level in RNE reflects almost complete depletion of GSH. Concerning the daily PO exposures, this condition was reached at ≥100 ppm. At lower PO exposure concentrations, NPSH depletion did not reach its minimum value and there was no cell proliferation. When the GSH precursor NAC was administered during exposures to 300 ppm PO, total NPSH depletion was prevented and PO elicited cell proliferation in RNE was abrogated. In agreement with the hypothesis of Lee et al. (2005), induction of cell proliferation in RNE should result from GSH depletion solely, independently of the GSH depleting PO. The appropriateness of this idea was shown by using the GSH depleting agents DEM and BSO. DEM is an electrophile that conjugates with GSH in the presence of GSH S-tranferases (Plummer et al., 1981) thus acting through a similar mechanism like PO, whereas BSO depletes GSH by irreversibly inhibiting γ glutamylcysteine synthetase, the rate-limiting enzyme in GSH synthesis (Griffith and Meister, 1979). Concerning NPSH status and cell proliferation, dosage of 2x250 mg/kg/day DEM resembled inhalation exposure to 50 ppm PO. The time-

courses of the NPSH levels were similar, NPSH was not depleted to its maximum, and cell proliferation was not increased. In contrast, administration of 500+150 mg/kg/day DEM resembled exposures to ≥100 ppm PO: At similar time-courses of the NPSH levels, NPSH depletion was maximum and cell proliferation was significantly increased. BSO treatment was also effective in maximum depleting NPSH in RNE but, in contrast to PO exposures and DEM treatments, no repletion was observed. The sustained maximum NPSH depletion during the last two days of observation reflects the irreversible inhibition of GSH synthesis. As with exposures ≥100 ppm PO and treatment with 500+150 mg/kg/day DEM, the maximum NPSH depletion was associated with increased cell proliferation. These findings demonstrate more generally the linkage between complete GSH depletion and cell proliferation in RNE.

One important physiological function of GSH is to protect the cell against various oxidants. Therefore, depletion of cellular GSH results in redox imbalance and oxidative stress. Redox imbalance in turn is widely accepted to be involved in both stimulated cell proliferation and cell death (Burdon, 1995; Matés et al., 2008; Genestra, 2007). An altered GSH-to-GSSG equilibrium has been suggested to play a specific signaling role in redox regulated proliferative and antiproliferative responses (Aw, 2003; Burdon, 1995; Fratelli et al., 2005). The proliferative response is considered to result from the activation of redox sensitive transcription factors such as nuclear factor kappa B (NF-κB) and Activator Protein-1 (AP-1) (Shaulian and Karin, 2001, 2002; Shukla et al., 2004; Valko et al., 2006). NF-κB is a heterodimer between Rel and p50 proteins. In the inactivated state, NF-κB is located in the cytosol and complexed with the inhibitory protein IκB. The activation of NF-κB is initiated by a signal-induced degradation of IκB. The degradation of IκB is induced by its phosphorylation by a specific kinase (IKK). As a result, IκB is ubiquitinated, dissociates from NF-

κB, and is degraded by the proteosome. The free NF-κB then translocates into the nucleus where it binds to specific DNA sequences, thereby leading to the transcription of target genes (reviewed in, e.g, Brasier, 2006; Gilmore, 2006; Perkins, 2007). AP-1 is composed of homodimers of Jun proteins (c-Jun, JunB, and JunD) or heterodimers of Jun and Fos (c-Fos, FosB, Fra1, and Fra2) proteins. The transactivation of AP-1 is mediated by the amino-terminal phosphorylation of c-Jun by the c-Jun N-terminal kinases (JNKs; reviewed in e.g., Reddy and Mossman, 2002). Induction of components of the AP-1 complex, namely c-Jun and c-Fos was shown in vitro as a result of reduced GSH-to-GSSG ratio (Tormos et al., 2004). Treatment of cells with DEM and BSO resulted in induction of AP-1 components Fos and FosB (Fratelli et al., 2005). In the rat liver, the GSH depleting agent phorone induced the expression of the AP-1 component c-jun (Oguro et al., 1998). However, redox imbalance mediated effects on cell proliferation and apoptosis appear to depend on a multitude of parameters such as cell type and source and extent of the redox imbalance (Cotgreave and Gerdes, 1998). Even subtoxic oxidative stress and mild redox shifts are discussed to stimulate cell proliferation (Aw, 2003; Cotgreave and Gerdes, 1998; Dypbukt et al., 1994). Obviously, rat RNE in vivo is relatively resistant to moderate intracellular redox imbalance with regard to cell turnover, because mild NPSH depletion, as has been observed after PO exposure to 50 ppm and treatment with 2x250 mg/kg/day DEM, did not stimulate cell replication. Drastic interference with the redox balance, i.e. severe daily perturbations of the NPSH status, was required to initiate cellular proliferation in RNE. In the case of PO, an additional proliferative stimulus – may be direct irritancy of inhaled PO (Rowe et al., 1956) – likely exists because cell proliferation increased with increasing exposure concentrations, despite maximum NPSH depletion at concentrations ≥100 ppm PO.

4.2 Relevance of cell proliferation for tumorigenesis in the respiratory nasal epithelium

Increased cell proliferation is generally regarded as a critical event in multi step carcinogenesis. Particularly in organs with low basal cell replication rates like RNE, the stimulation of a proliferative response is assumed to be a major risk factor for the development of cancer (Cohen and Ellwein, 1990, 1991; Monticello and Morgan, 1997).

In rats exposed up to 50 ppm PO, cell proliferation in RNE did not differ from the control value (this work; Eldridge et al., 1995; Ríos-Blanco et al., 2003b). At 100 and 200 ppm PO, S-phase positive cells in RNE were statistically significantly increased (this work). Eldridge et al. (1995) did not find significantly increased cell proliferation at 150 ppm PO, possibly due to the high standard error. At 300 ppm PO (this study; Ríos-Blanco et al., 2003b) and 525 ppm PO (Eldridge et al., 1995), cell replication rate was more than 3-fold the control value. The present results, in agreement with those of Eldridge et al. (1995) and Ríos-Blanco et al. (2003b), unequivocally demonstrate a nonlinear response for PO induced cell proliferation in rat RNE with a no-observed-effect level (NOEL) of 50 ppm PO.

At PO concentrations of 100 and 200 ppm, the statistically significantly increased cell proliferation in total RNE resulted from cell proliferation in the mucociliary epithelium lining the septum, the dorsal medial meatus, and the medial surface of the nasoturbinates. The transitional epithelium of the lateral surface of the nasoturbinates in the ventral-lateral part of which tumors had been developed at PO concentrations of ≥300 ppm, showed statistically significantly increased cell proliferation only at a PO concentration of 300 ppm. Consequently, the NOEL for cell proliferation in the epithelium where tumors had developed is 200 ppm PO. Observations from Ríos-Blanco et al. (2003b)

support the present findings to that effect that the increase in cell proliferation following PO inhalation exposure is more pronounced in the mucociliary than in the transitional epithelium. The authors reported increase in cell proliferation in the transitional epithelium of the nasoturbinates at 300 ppm PO, which, however, was statistically significant only after 20 days of exposure.

The question arises why the proliferative response in RNE upon PO inhalation exposure is site specific. The regional deposition of a chemical in the nose and local tissue susceptibility are major factors for the distribution of lesions in the respiratory tract (Morgan and Monticello, 1990). Airflow patterns play an important role in the regional deposition of a chemical in the nose. Airflow was calculated to be higher in the transitional than in the mucociliary epithelium of the nasal respiratory tissue (Kimbell et al., 1997). Thus, the airflow does not correlate with the regions with the highest proliferation rates. A physiological toxicokinetic model for inhaled PO (Csanády and Filser, 2007) showed the steady-state distribution between PO in air and in respiratory epithelium to be reached almost immediately. Since, according to this model, the uptake of PO is controlled only by diffusion, it was concluded that the tissue concentration of PO in RNE was the same in both the mucociliary and the transitional epithelium (Csanády and Filser, 2007). Therefore, the higher proliferation rate in the mucociliary epithelium of PO exposed rats can hardly be explained by kinetic parameters. Tissue susceptibility seems to be the key factor for the observed differences. Our study and the previous one from Ríos-Blanco et al. (2003b) did not detect any treatment related histopathological changes in both types of the epithelium after 3 days of exposure at any of the PO concentrations tested. After longer exposure periods to PO concentrations ≥150 ppm, epithelial lesions were found (Eldridge et al., 1995; Ríos-Blanco et al., 2003b). These were restricted to the mucociliary epithelium and included mainly hyperplasia or

hypertrophy of mucous cells. The preferential induction of cell proliferation in the mucociliary epithelium might reflect a regenerative response to the irritancy of PO (Rowe et al., 1956) in addition to a response mediated by GSH depletion. Also other gaseous irritants such as formaldehyde and glutaraldehyde have been reported to induce nasal mucous cell hyperplasia or hypertrophy (Chang et al., 1983; Monteiro-Riviere and Popp, 1986; St. Clair et al., 1990). The relevance of irritation on cell proliferation in the mucociliary epithelium is also supported by the finding that treatment of the animals with the GSH depleting substances DEM or BSO resulted in homogenously distributed induced cell proliferation in RNE without preference for the mucociliary epithelium. One should not expect these substances to have any irritant effects on RNE following ip administration.

4.3 Site specificity of propylene oxide induced tumors in the respiratory nasal epithelium

It is unclear why PO induced tumors developed in the transitional epithelium and not in the mucociliary epithelium despite high induction of cell proliferation. PO related genotoxic effects might be crucial. The predominant N7-substituted guanines are considered non mutagenic as they are unstable and are removed by spontaneous depurination, leading to apurinic sites, which are efficiently repaired. In contrast, the by far minor adducts N1- and N^6-HPA as well as the N3-cytosine adducts (forming by hydrolytic deamination the detected N3-HPU; Koskinen and Plná, 2000) are potentially promutagenic (Albertini and Sweeney, 2007). Beside PO related direct genotoxicity, genotoxic effects could also result from oxidative stress induced by depletion of GSH. In agreement, increased oxidative DNA damage has been reported following GSH depletion (Green et al., 2006; Higuchi, 2004; Reliene and Schiestl, 2006).

Moreover, GSH depletion seems to impair DNA repair capacity (Langie et al., 2007). A recent study revealed marked differences in the antioxidative status within rat RNE (Reed et al., 2003). The authors demonstrated by immunohistochemical techniques the antioxidative enzymes GSH-peroxidase, catalase, Mn-superoxide dismutase, Cu/Zn-superoxide dismutase, and DT-diaphorase to be localized in the ciliated cells of the RNE and not in the transitional epithelium of the nasoturbinates. This implies a lower ability of the transitional epithelium to counteract oxidative stress evoked by GSH depletion and a higher susceptibility of this tissue for oxidative DNA modifications. Hence, a preferential accumulation of possible oxidative DNA damage in the transitional epithelium could account for the site-specific development of nasal tumors upon PO inhalation exposure.

4.4 General conclusion

The present results confirm the hypothesis (Lee et al., 2005) that GSH depletion in rat RNE should induce cell proliferation. Considering cell proliferation to be a prerequisite for PO induced nasal tumor formation, it follows that the GSH status in RNE is of utmost importance for nasal tumorigenicity of PO in rats.

4.5 Outlook

Before the findings in the rat can be transferred to the human situation, their general relevance has to be evaluated in another animal species. Therefore, it will be investigated whether there exists also in PO exposed mice a conjunction between GSH depletion and cell proliferation in RNE. In this species, PO induced nasal tumorigenesis was accompanied by hyperplasia, too. Provided that the mouse studies corroborate the results of the present study, it will be

justified to account for the GSH status in humans when assessing a cancer risk from inhalation exposure to PO.

5 SUMMARY

English

Propylene oxide (PO) is a high volume chemical used primarily in the production of polyurethane polyols, propylene glycols, glycol ethers, and specialty chemicals. The main route of human exposure to PO occurs by inhalation at the workplace. In rodents, PO is a site of contact carcinogen. After PO inhalation exposure of Fischer 344 rats, tumors were observed in respiratory nasal epithelium (RNE) at exposure concentrations ≥300 ppm but not at 0, 100, or 200 ppm PO. The compound reacts directly with DNA forming mainly the N7-(2-hydoxypropyl) guanine (N7-HPG) adduct. The PO concentration-dependent increase in N7-HPG adducts in RNE was linear and did not parallel with the exposure response for tumor formation. Therefore, it was suggested that PO induced nasal tumorigenicity should not result solely from the genotoxicity of PO. Previous studies in rats exposed by inhalation to 0, 5, 10, 20, 25, 50, 150, 300, 500, or 525 ppm PO for 3 days (6 h/day) and up to 4 weeks (6 h/day, 5 days/week) demonstrated statistically significant increased cell proliferation in rat RNE at PO concentrations ≥300 ppm. Also, a loss of the glutathione (GSH) content in this tissue, measured as water-soluble non-protein thiol (NPSH), was shown. The decline of cellular GSH was attributed to glutathione S-transferase mediated PO conjugation with GSH. Combining the findings on PO dependent tumor formation, genotoxicity, cell proliferation, and NPSH status in RNE as well as on metabolism and kinetics of PO in RNE, it was hypothesized that repeated and severe perturbation of GSH, resulting from metabolic PO elimination, was the molecular cause of PO induced cell proliferation, which was considered as critical step on the path to tumors in rat RNE. The goal of the present study was to investigate by means of different

approaches whether GSH depletion in RNE induces cell proliferation in this tissue in dependence on the PO concentration and, in addition, independently thereof. First, NPSH status and cell proliferation in RNE were studied in Fischer 344 rats after 3 days of inhalation exposure (6 h/day) to 0, 50, 100, 200, or 300 ppm PO. Second, it was tested whether PO induced NPSH depletion and cell proliferation could be prevented by simultaneously administering (sc) the GSH precursor N-acetylcysteine (NAC; 2x500 mg/kg/day). Third, it was investigated whether NPSH depletion as such could result in cell proliferation in RNE by treating rats systemically (ip) with the GSH depleting agents diethylmaleate (DEM; 2x250 mg/kg/day, 3 days or 500+150 mg/kg/day, 3 days) and L-buthionine sulfoximine (BSO; 500 mg/kg/day, 3 days). DEM is an electrophile that conjugates with GSH in the presence of GSH S-tranferases thus acting through a similar mechanism like PO, whereas BSO depletes GSH by irreversibly inhibiting γ-glutamylcysteine synthetase, the rate-limiting enzyme in GSH synthesis. NPSH concentrations in RNE were quantified using the Ellman's assay. Cell proliferation was evaluated by immunohistochemical detection of bromodeoxyuridine (BrdU) incorporation into DNA. The number of positive cells per mm of basement membrane (Unit Length Labeling Index; ULLI) was used to quantify BrdU incorporation.

Exposure to 50 ppm PO resulted in partial NPSH depletion of approximately 50% of the mean control value. At concentrations of ≥100 ppm PO, NPSH levels were around their minimum, about 25% of the control value. The residual NPSH reflected mitochondrial GSH and cystein which was formed from GSH during the surgical procedure. Therefore, the residual cytosolic NPSH level in RNE of approximately 25% reflected almost complete depletion of cytosolic GSH. At 50 ppm PO, cell proliferation in RNE did not differ from the control value. At 100, 200, and 300 ppm PO, cell proliferation was statistically

significantly and concentration-dependently increased up to 3.7-fold the control value. The present results demonstrate that increased cell proliferation in RNE occurred only when NPSH was around its minimum with a no-observed-effect level (NOEL) for cell proliferation of 50 ppm PO. However, in addition to maximum NPSH depletion at concentrations ≥100 ppm PO, a further proliferative stimulus - likely the direct irritancy of inhaled PO – seems to exist because cell proliferation increased with increasing PO exposure concentrations. At PO concentrations of 100 ppm and above, the increased cell proliferation was observed in the mucociliary epithelium. The transitional epithelium of the lateral surface of the nasoturbinates in the ventral-lateral part of which tumors had been developed, showed statistically significantly increased cell proliferation only at a PO concentration of 300 ppm. Consequently, the NOEL for cell proliferation in the epithelium where tumors had developed is 200 ppm PO.

The causal relation between NPSH status and cell proliferation in rat RNE is substantiated by the results obtained after treatment with NAC, DEM, and BSO. When the GSH precursor NAC was administered during exposures to 300 ppm PO, maximum NPSH depletion was prevented and PO elicited cell proliferation was abrogated. DEM at a dose of 2x250 mg/kg/day resembled inhalation exposure to 50 ppm PO concerning both NPSH status and cell proliferation: The time-courses of the NPSH levels were similar, NPSH levels did not decline to the minimum value, and cell proliferation did not differ from controls. In contrast, administration of 500+150 mg/kg/day DEM resembled exposures to ≥100 ppm PO: At similar time-courses of the NPSH levels, NPSH levels were at their minimum and cell proliferation was significantly increased. BSO treatment was also effective in maximum depleting NPSH in RNE and this was associated with increased cell proliferation.

The present results confirm the hypothesis that repeated and severe perturbation of GSH levels in rat RNE should induce cell proliferation. Considering cell proliferation to be a prerequisite for PO induced nasal tumor formation, it follows that the GSH status in RNE is of utmost importance for nasal tumorigenicity of PO in rats.

German

Propylenoxid (PO), eine in großen Mengen hergestellte Industriechemikalie, dient hauptsächlich zur Produktion von Polyurethanpolyolen, Propylenglykolen, Glykolethern und Spezialchemikalien. Die Exposition des Menschen gegen PO findet hauptsächlich am Arbeitsplatz durch Inhalation statt. Beim Nagetier wirkt PO am Applikationsort tumorigen.

PO reagiert direkt mit der DNA, hauptsächlich unter Bildung von N7-(2-hydoxypropyl)guanin (N7-HPG). Bei PO-exponierten Fischer-344-Ratten nahm die N7-HPG-Adduktbildung im respiratorischen Nasenepithel (RNE) linear mit der Stoffkonzentration in der Atemluft zu. Tumore im RNE entwickelten sich nach Langzeitexposition nur bei hohen PO-Konzentrationen (≥300 ppm). Aufgrund dieser unterschiedlichen Dosis-Wirkungsbeziehungen wurde vermutet, dass die PO-bedingte Tumorigenität im RNE nicht allein auf die Genotoxizität von PO zurückzuführen sei. Frühere Untersuchungen an Ratten, die gegen 0, 5, 10, 20, 25, 50, 150, 300, 500 und 525 ppm PO drei Tage lang (6 h/Tag) und bis zu 4 Wochen (6 h/Tag, 5 Tage/Woche) exponiert waren, zeigten erhöhte Zellproliferation im RNE, jedoch erst bei PO-Konzentrationen ≥300 ppm. Außerdem wurde ein Abfall des Gehalts an Glutathion (GSH) – gemessen als wasserlösliches Nicht-Protein-Thiol (NPSH) – im gleichen Gewebe gefunden. Dieser Effekt wurde auf die GSH-S-Transferase katalysierte Konjugation von GSH mit PO zurückgeführt. Vor dem Hintergrund der

Erkenntnisse zur PO-abhängigen Tumorigenität, Genotoxizität, Zellproliferation und dem NPSH-Status sowie der Informationen zur Toxikokinetik von PO im RNE wurde folgende Hypothese aufgestellt: Wiederholte und massive Störung der GSH-Homöostase im RNE aufgrund der PO-GSH-Konjugation führt in diesem Gewebe zu erhöhter Zellproliferation, welche einen essentiellen Schritt für die PO-abhängige Tumorigenität im Ratten-RNE darstellt. Die Arbeit hatte zum Ziel, zu überprüfen, ob abhängig von PO und unabhängig davon eine Störung der GSH-Homöostase im RNE Zellproliferation in diesem Gewebe induziert. Zum einen sollten NPSH-Status und Zellproliferation im RNE von Fischer-344-Ratten nach 3-tägigen Expositionen gegen 0, 50, 100, 200 bzw. 300 ppm PO bestimmt werden. Zum anderen sollte ermittelt werden, ob PO-abhängige NPSH-Depletion und Zellproliferation im RNE durch subkutane Verabreichung des GSH-Vorläufers N-Acetylcystein (NAC; 2x500 mg/kg/Tag, 3 Tage) unterbunden werden könne. Schließlich war zu untersuchen, ob auch eine PO-unabhängige NPSH-Depletion im RNE zu erhöhter Zellproliferation in diesem Gewebe führen könne. Hierzu sollten Ratten intraperitoneal mit den GSH-Depletoren Diethylmaleat (DEM; 2x250 mg/kg/Tag bzw. 500+150 mg/kg/Tag, jeweils 3 Tage) und Buthioninsulfoximin (BSO; 500 mg/kg/Tag, 3 Tage) behandelt werden. Das elektrophile DEM konjugiert wie PO an GSH in Gegenwart der GSH-S-Transferase. BSO hingegen depletiert GSH durch irreversible Hemmung der γ-Glutamylcysteinsynthetase, des geschwindigkeitsbestimmenden Enzyms der GSH-Synthese. Der NPSH-Gehalt sollte mit dem Ellman-Test bestimmt werden. Die Zellproliferation sollte immunhistochemisch über den Einbau von Bromdesoxyuridin (BrdU) in die DNA untersucht werden. Als quantitatives Maß hierfür sollte die Anzahl der markierten Zellen pro mm Basalmembran („Unit Length Labeling Index“; ULLI) herangezogen werden.

Expositionen gegen 50 ppm PO führten zu einer partiellen NPSH-Depletion von etwa 50% des Kontrollwerts. Bei ≥100 ppm PO wurde die maximale NPSH-Depletion erreicht, die bei 25% des Kontrollwerts lag. Das verbleibende NPSH dürfte mitochondriales GSH repräsentieren oder Cystein, das während der Präparation des RNE aus GSH entsteht. Somit sollte der NPSH Gehalt bei ≥100 ppm PO einer vollständigen Depletion von zytosolischem GSH entsprechen. Die Zellproliferation unterschied sich bei 50 ppm PO nicht statistisch signifikant vom Kontrollwert, nahm jedoch bei PO Konzentrationen ≥100 ppm statistisch signifikant, konzentrationsabhängig zu und erreichte bei 300 ppm das 3,7-fache des Kontrollwerts.

Applikation des GSH-Vorläufers NAC und gleichzeitige Exposition gegen 300 ppm PO resultierte nicht in einer maximalen NPSH-Depletion im RNE, und die Zellproliferation war nicht erhöht. DEM, in einer Dosis von 2x250 mg/kg/Tag, ähnelte der Exposition gegen 50 ppm insofern, dass der NPSH-Gehalt nur teilweise abfiel und es nicht zu einer erhöhten Zellproliferation kam. Bei einer DEM-Dosis von 500+150 mg/kg/Tag und nach Behandlung mit BSO hingegen kam es zur maximalen NPSH-Depletion und erhöhten Zellproliferation, ähnlich wie nach Exposition gegen ≥100 ppm PO.

Die Ergebnisse zeigen, dass im RNE nur dann erhöhte Zellproliferation auftritt, wenn der NPSH-Gehalt in diesem Gewebe maximal depletiert ist. Im Fall von PO muss ein zusätzlicher Stimulus für Zellproliferation existieren, da, trotz maximaler NPSH-Depletion bei ≥100 ppm PO, die Zellproliferation mit zunehmender PO-Konzentration weiterhin ansteigt. Hierbei handelt es sich wahrscheinlich um die direkte Reizwirkung von PO. Die erhöhte Zellproliferation betraf vor allem das mukoziliäre Epithel. Erst bei 300 ppm PO zeigte auch das Übergangsepithel, in dem die PO-induzierten Tumore gefunden wurden, erhöhte Zellproliferation. Somit liegen die „No-observed-

effect levels“ für die PO-induzierte Zellproliferation für das Übergangsepithel bei 200 ppm PO und für das RNE insgesamt bei 50 ppm PO. Vor dem Hintergrund, dass erhöhte Zellproliferation als Voraussetzung für die PO-induzierte Tumorigenität im RNE der Ratte angesehen wird, ist abzuleiten, dass die GSH-Homöostase im RNE von höchster Bedeutung für die Tumorigenität von PO ist.

6 ABBREVIATIONS

ANOVA	Analysis of variance
AP-1	Activator Protein-1
BrdU	5-Bromodeoxyuridine
BSO	Buthionine sulfoximine
DEM	Diethylmaleate
EH	Epoxyhydrolase
GC	Gas chromatograph
GSH	Reduced glutathione
GSSG	Oxidized glutathione
GST	Glutathione S-transferase
N1-HPA	N1-(2-hydroxypropyl)adenine
N^6-HPA	N^6-(2-hydroxypropyl)adenine
N7-HPG	N7-(2-hydroxypropyl)guanine
N3-HPU	N3-(2-hydroxypropyl)uracil
ip	Intraperitoneal
NAC	N-acetylcysteine
NPSH	Non-protein thiol
NOEL	No-observed-effect level
NFκB	Nuclear factor kappa B
PO	Propylene oxide
ppm	Parts per million
RNE	Respiratory nasal epithelium
sc	Subcutaneous
w.w.	Wet weight

7 REFERENCES

Agurell, E., Cederberg, H., Ehrenberg, L., Lindahl-Kiessling, K., Rannug, U., Törqvist, M., 1991. Genotoxic effects of ethylene oxide and propylene oxide: a comparative study. Mutat. Res. 250, 229-237.

Albertini, R.J., Sweeney, L.M., 2007. Propylene oxide: genotoxicity profile of a rodent nasal carcinogen. Crit. Rev. Toxicol. 37, 489-520.

Anderson, M.E., 1998. Glutathione: an overview of biosynthesis and modulation. Chem. Biol. Interact. 11-112, 1-14.

ACGIH, 2008. American Conference of Govermental Industrial Hygienists. TLVs® and BEIs®. Threshold Limit Values for Chemical Substances and Physical Agents and Biological Exposure Indices. Cincinnati, Ohio, USA.

Aw, T.Y., 2003. Cellular redox: a modulator of intestinal epithelial cell proliferation. News Physiol. Sci. 18, 201-204.

Bailey, E., Farmer, P.B., Shuker, D.E., 1987. Estimation of exposure to alkylating carcinogens by the GC-MS determination of adducts to hemoglobin and nucleic acid bases in urine. Arch. Toxicol. 60, 187-191.

Ball, L., Jones, A., Boogaard, P., Will, W., Aston, P., 2005. Development of a competitive immunoassay for the determination of N-(2-hydroxypropyl)-valine adducts in human haemoglobin and its application in biological monitoring. Biomarkers 10, 127-137.

Boogaard, P.J., Rocchi, P.S., van Sittert, N.J., 1999. Biomonitoring of exposure to ethylene oxide and propylene oxide by determination of hemoglobin adducts: Correlations between airborne exposure and adduct levels. Int. Arch. Occup. Environ. Health 72, 142-150.

Boorman, G.A., Morgan, K.T., Uriah, L.C., 1990. Nose, larynx, and trachea. In: Pathology of the Fischer Rat (G.A. Boorman, Ed.), pp. 315-337. Academic Press, San Diego.

Bootman, J., Lodge, D.C., Whalley, H.E., 1979. Mutagenic activity of propylene oxide in bacterial and mammalian systems. Mutat. Res. 67, 101-112.

Brasier, A.R., 2006. The NF-kappaB regulatory network. Cardiovasc. Toxicol. 6, 111-130.

Burdon, R.H., 1995. Superoxide and hydrogen peroxide in relation to mammalian cell proliferation. Free Radic. Biol. Med. 18, 775-794.

Carpenter, C.P., Smyth, H.F., 1946. Chemical burns of the rabbit cornea. Am. J. Ophthalmol. 29, 1363-1372.

Casanova-Schmitz, M., Starr, T.B., Heck, H.D., 1984. Differentiation between metabolic incorporation and covalent binding in the labeling of macromolecules in the rat nasal mucosa and bone marrow by inhaled [^{14}C]- and [^{3}H]formaldehyde. Toxicol. Appl. Pharmacol. 76, 26-44.

Chang, J.C., Gross, E.A., Swenberg, J.A., Barrow, C.S., 1983. Nasal cavity deposition, histopathology, and cell proliferation after single or repeated formaldehyde exposures in B6C3F1 mice and F-344 rats. Toxicol. Appl. Pharmacol. 68, 161-176.

Cohen, S.M., Ellwein, L.B., 1990. Cell proliferation in carcinogenesis. Science 249, 1007-1011.

Cohen, S.M., Ellwein, L.B., 1991. Genetic errors, cell proliferation, and carcinogenesis. Cancer Res. 51, 6493-6505.

Comporti, M., 1989. Three models of free radical-induced cell injury. Chem. Biol. Interact. 72, 1-56.

Cotgreave, I.A., Gerdes, R.G., 1998. Recent trends in glutathione biochemistry–glutathione-protein interactions: A molecular link between oxidative stress and cell proliferation? Biochem. Biophys. Res. Commun. 242, 1-9.

Csanády, G.A., Filser, J.G., 2007. A physiological toxicokinetic model for inhaled propylene oxide in rat and human with special emphasis on the nose. Toxicol. Sci. 95, 37-62.

Czène, K., Osterman-Golkar, S., Yun, X., Li, G., Zhao, F., Pérez, H.L., Li, M., Natarajan, A.T., Segerbäck, D., 2002. Analysis of DNA and hemoglobin adducts and sister chromatid exchanges in a human population occupationally exposed to propylene oxide: A pilot study. Cancer Epidemiol. Biomarkers Prev. 11, 315-318.

DeLeve, L.D., Kaplowitz, N., 1991. Glutathione metabolism and its role in hepatotoxicity. Pharmacol. Ther. 52, 287-305.

DFG, 1996. Deutsche Forschungsgemeinschaft. Gesundheitsschädliche Arbeitsstoffe. Toxikologisch-arbeitsmedizinische Begründung von MAK-Werten, 23. Lieferung, Wiley-VCH, Weinheim.

Djuric, Z., Hooberman, B.H., Rosman, L., Sinsheimer, J.E., 1986. Reactivity of mutagenic propylene oxides with deoxynucleosides and DNA. Environ. Mutagen. 8, 369-383.

Dunkelberg, H., 1981. Carcinogenic activity of ethylene oxide and its reaction products 2-chloroethanol, 2-bromoethanol, ethylene glycol and diethylene glycol. I. Carcinogenicity of ethylene oxide in comparison with 1,2-propylene oxide after subcutaneous administration in mice. Zentralbl. Bakteriol. Mikrobiol. Hyg. [B] 174, 383-404.

Dunkelberg, H., 1982. Carcinogenicity of ethylene oxide and 1,2-propylene oxide upon intragastric administration to rats. Br. J. Cancer 46, 924-933.

Dypbukt, J.M., Ankarcrona, M., Burkitt, M., Sjöholm, A., Ström, K., Orrenius, S., Nicotera, P., 1994. Different prooxidant levels stimulate growth, trigger apoptosis, or produce necrosis of insulin-secreting RINm5F cells. The role of intracellular polyamines. J. Biol. Chem. 269, 30553-30560.

EC, 2002. European Commission, Joint Research Centre. EINECS No.: 200-879-2; Summary Risk Assessment Report, Methyloxirane (Propylene oxide), Special Publication 1.02.129; © European Communities, 2002.

Eldridge, S.R., Bogdanffy, M.S., Jokinen, M.P., Andrews, L.S., 1995. Effects of propylene oxide on nasal epithelial cell proliferation in F344 rats. Fundam. Appl. Toxicol. 27, 25-32.

Faller, T.H., Csanády, G.A., Kreuzer, P.E., Baur, C.M., Filser, J.G., 2001. Kinetics of propylene oxide metabolism in microsomes and cytosol of different organs from mouse, rat, and humans. Toxicol. Appl. Pharmacol. 172, 62-74.

Farmer, P.B., Gorf, S.M., Bailey, E., 1982. Determination of hydroxypropylhistidine in haemoglobin as a measure of exposure to propylene oxide using high resolution gas chromatography mass spectrometry. Biomed. Mass Spectrom. 9, 69-71.

Farooqi, Z., Törnqvist, M., Ehrenberg, L., Natarajan, A. T., 1993. Genotoxic effects of ethylene oxide and propylene oxide in mouse bone marrow cells. Mutat. Res. 288, 223-228.

Filser, J.G., 1992. The closed chamber technique–uptake, endogenous production, excretion, steady-state kinetics and rates of metabolism of gases and vapors. Arch. Toxicol. 66, 1-10.

Fjellstedt, T.A., Allen, R.H., Duncan, B.K., Jakoby, W.B., 1973. Enzymatic conjugation of epoxides with glutathione. J. Biol. Chem. 248, 3702-3707.

Fratelli, M., Goodwin, L.O., Ørom, U.A., Lombardi, S., Tonelli, R., Mengozzi, M., Ghezzi, P., 2005. Gene expression profiling reveals a signaling role of glutathione in redox regulation. Proc. Natl. Acad. Sci. U.S.A. 102, 13998-14003.

Genestra, M., 2007. Oxyl radicals, redox-sensitive signalling cascades and antioxidants. Cell Signal. 19, 1807-1819.

Giri, A.K., 1992. Genetic toxicology of propylene oxide and trichloropropylene oxide — A review. Mutat. Res. 277, 1-9.

Gilmore, T.D., 2006. Introduction to NF-κB: players, pathways, perspectives. Oncogene 25, 6680-6684.

Golka, K., Peter, H., Denk, B., Filser, J.G., 1989. Pharmacokinetics of propylene and its reactive metabolite propylene oxide in Sprague-Dawley rats. Arch. Toxicol. Suppl. 13, 240-242.

Green, R.M., Graham, M., O'Donovan, M.R., Chipman, J.K., Hodges, N.J., 2006. Subcellular compartmentalization of glutathione: correlations with parameters of oxidative stress related to genotoxicity. Mutagenesis 21, 383-390.

Griffith, O.W., Meister, A., 1979. Potent and specific inhibition of glutathione synthesis by buthionine sulfoximine (S-n-butyl homocysteine sulfoximine). J. Biol. Chem. 254, 7558-7560.

Guengerich, F., Mason, P., 1980. Alcohol dehydrogenase-coupled spectrophotometric assay of epoxide hydratase activity. Anal. Biochem. 104, 445-451.

Hardin, B.D., Schuler, P.M., McGinnis, P.M., Niemeier, R.W., Smith, R.J., 1983. Evaluation of propylene oxide for mutagenic activity in 3 in vivo test systems. Mutat. Res. 117, 337-344.

Higuchi, Y., 2004. Glutathione depletion-induced chromosomal DNA fragmentation associated with apoptosis and necrosis. J. Cell. Mol. Med. 8, 455-464.

Hine, C.H., Rowe, V.K., White, E.R., Darmer, K.I., Youngblood, G.T., 1981. Epoxy compounds. In: Patty's Industrial Hygiene and Toxicology (G.D. Clayton and F.E. Clayton, Eds.), third edition, Vol. 2A, pp. 2141-2257. Interscience Publishers, John Wiley & Sons, New York.

Högstedt, B., Bergmark, E., Törnqvist, M., Osterman-Golkar, S., 1990. Chromosomal aberrations and micronuclei in lymphocytes in relation to alkylation of hemoglobin in workers exposed to ethylene oxide and propylene oxide. Hereditas 113, 133-138.

IARC, 1994 International Agency for Research on Cancer (IARC). IARC monographs on the evaluation of carcinogenic risks to humans, Vol. 60: Some industrial chemicals. IARC, Lyon.

Jacobson, K.H., Hackley, E.B., Feinsilver, L., 1956. The toxicity of inhaled ethylene oxide and propylene oxide vapours. Arch. ind. Health 13, 237-244.

Jensen, O., 1981. Contact allergy to propylene oxide and isopropyl alcohol in a skin disinfactant swab. Contact Dermatitis 7, 148-150.

Jones, A.L., Van der Woord, M., Bourrillon, F., 2005. Use of a whole blood competitive immunoassay for the assessment of worker exposures to propylene oxide at three manufacturing facilities. Ann. Occup. Hyg. 49, 241-243.

Kimbell, J.S., Godo, M.N., Gross, E.A., Joyner, D.R., Richardson, R.B., Morgan, K.T., 1997. Computer simulation of inspiratory airflow in all regions of the F344 rat nasal passages. Toxicol. Appl. Pharmacol. 145, 388-398.

Kolman, A., Spivak, I., Naslund, M., Dusinska, M., Cedervall, B., 1997. Propylene oxide and epichlorohydrin induce DNA strand breaks in human diploid fibroblasts. Environ. Mol. Mutagen. 30, 40-46.

Kolman, A., Chovanec, M., Osterman-Golkar, S., 2002. Genotoxic effects of ethylene oxide, propylene oxide and epichlorohydrin in humans: Update review (1990–2001). Mutat. Res. 512, 173-194.

Koskinen, M., Plná, K., 2000. Specific DNA adducts induced by some mono-substituted epoxides in vitro and in vivo. Chem. Biol. Interact. 129, 209-229.

Kuper, C.F., Reuzel, P.G., Feron, V.J., Verschuuren, H., 1988. Chronic inhalation toxicity and carcinogenicity study of propylene oxide in Wistar rats. Food Chem. Toxicol. 26, 159-167.

Kwon, Y.H., Jovanovic, A., Serfas, M.S., Tyner, A.L., 2003. The Cdk inhibitor p21 is required for necrosis, but it inhibits apoptosis following toxin-induced liver injury. J. Biol. Chem. 278, 30348-30355.

Langie, S.A., Knaapen, A.M., Houben, J.M., van Kempen, F.C., de Hoon, J.P., Gottschalk, R.W., Godschalk, R.W., van Schooten, F.J., 2007. The role of glutathione in the regulation of nucleotide excision repair during oxidative stress. Toxicol. Lett. 168, 302-309.

Lawley, P.D., Jarman, M., 1972. Alkylation by propylene oxide of deoxyribonucleic acid, adenine, guanosine and deoxyguanylic acid. Biochem. J. 126, 893-900.

Lee, M.S., Dhawan, M., Faller, T., Kessler, W., Filser, J.G., 1998. Propene oxide in blood and glutathione depletion in nose, lung, and liver of rats exposed to propene oxide. Naunyn-Schmiedeberg's Arch. Pharmacol. Suppl. 357(4), R172.

Lee, M.S., Dhawan-Robl, M., Faller, T.H., Csanády, Gy. A., Kessler, W., Filser J.G., 2000. Propylene oxide in blood and glutathione levels in tissues of rats exposed up to 4 weeks to different concentrations of gaseous propylene oxide. Naunyn-Schmiedeberg's Arch. Pharmacol. Suppl. 361(4), R139.

Lee, M.S., Faller, T.H., Kreuzer, P.E., Kessler, W., Csanády, G.A., Pütz, C., Ríos-Blanco, M.N., Pottenger, L.H., Segerbäck, D., Osterman-Golkar, S., Swenberg, J.A., Filser, J.G., 2005. Propylene oxide in blood and soluble non-protein thiols in nasal mucosa and other tissues of male Fischer 344/N rats exposed to propylene oxide vapors-relevance of glutathione depletion for propylene oxide-induced rat nasal tumors. Toxicol. Sci. 83, 177-189.

Lynch, D.W., Lewis, T.R., Moorman, W.J., Burg, J.R., Groth, D.H., Khan, A., Ackerman, L.J., Cockrell, B.Y., 1984. Carcinogenic and toxicologic effects of inhaled ethylene oxide and propylene oxide in F344 rats. Toxicol. Appl. Pharmacol. 76, 69-84.

Lynch, D.W., Lewis, T.R., Moorman, W.J., Burg, J.R., Gulati, D.K., Kaur, P., Sabharwal, P.S., 1984a. Sister-chromatid exchanges and chromosome aberrations in lymphocytes from monkeys exposed to ethylene oxide and propylene oxide by inhalation. Toxicol. Appl. Pharmacol. 76, 85-95.

Matés, J.M., Segura, J.A., Alonso, F.J., Márquez, J., 2008. Intracellular redox status and oxidative stress: implications for cell proliferation, apoptosis, and carcinogenesis. Arch. Toxicol. 82, 273-299.

McGregor, D., Brown, A.G., Cattanach, P., Edwards, I., McBride, D., Riach, C., Sheperd, W., Caspary, W.J., 1991. Responses of the L5178Y mouse lymphoma forward mutation assay: V. Gases and vapors. Environ. Mol. Mutagen. 17, 122-129.

McLaughlin, R.S., 1946. Chemical burns of the human cornea. Am. J. Ophthalmol. 29, 1355-1362.

Monteiro-Riviere, N.A., Popp, J.A., 1986. Ultrastructural evaluation of acute nasal toxicity in the rat respiratory epithelium in response to formaldehyde gas. Fundam. Appl. Toxicol. 6, 251-262.

Monticello, T.M., Morgan, K.T., 1997. Chemically-induced nasal carcinogenesis and epithelial cell proliferation: a brief review. Mutat. Res. 380, 33-41.

Monticello, T.M., Morgan, K.T., Hurtt, M.E., 1990. Unit length as the denominator for quantitation of cell proliferation in nasal epithelia. Toxicol. Pathol. 18, 24-31.

Morgan, K.T., Monticello, T.M., 1990. Airflow, gas deposition, and lesion distribution in the nasal passages. Environ. Health Perspect. 88, 209-218.

Morris, J.B., Banton, M.I., Pottenger, L.H., 2004. Uptake of inspired propylene oxide in the upper respiratory tract of the F344 rat. Toxicol. Sci. 81, 216-224.

Morris, J.B., Pottenger, L.H., 2006. Propylene oxide uptake and nasal NPSH depletion in the upper respiratory tract of the mouse. Toxicol. Sci. 92, 228-34.

NTP, 1985. National Toxicology Program. Toxicology and carcinogenesis studies of propylene oxide in F344/N rats and B6C3F1 mice (inhalation studies). NTP TR 267. U.S. Department of Health and Human Services, Public Health Service, National Institutes of Health, Research Triangle Park, NC.

Oguro, T., Hayashi, M., Nakajo, S., Numazawa, S., Yoshida, T., 1998. The expression of heme oxygenase-1 gene responded to oxidative stress produced by phorone, a glutathione depletor, in the rat liver; the relevance to activation of c-jun n-terminal kinase. J. Pharmacol. Exp. Ther. 287, 773-778.

Ohnishi, A., Murai, Y., 1993. Polyneuropathy due to ethylene oxide, propylene oxide, and butylene oxide. Environ. Res., 60, 242-247.

Osterman-Golkar, S., Czène, K., Lee, M.S., Faller, T.H., Csanády, G.A., Kessler, W., Pérez, H.L., Filser, J.G., Segerbäck, D., 2003. Dosimetry by means of DNA and hemoglobin adducts in propylene oxide-exposed rats. Toxicol. Appl. Pharmacol. 191, 245-254.

Perkins, N.D., 2007. Integrating cell-signalling pathways with NF-κB and IKK function. Nat. Rev. Mol. Cell Biol. 8, 49-62.

Pero, R.W., Osterman-Golkar, S., Högstedt, B., 1985. Unscheduled DNA synthesis correlated to alkylation of hemoglobin in individuals occupationally exposed to propylene oxide. Cell. Biol. Toxicol. 1, 309-314.

Plná, K., Nilsson, R., Koskinen, M., Segerbäck, D., 1999. 32P-postlabelling of propylene oxide 1- and *N*(6)-substituted adenine and 3-substituted cytosine/uracil: formation and persistence in vitro and in vivo. Carcinogenesis 20, 2025-2032.

Plummer, J.L., Smith, B.R., Sies, H., Bend, J.R., 1981. Chemical depletion of glutathione in vivo. Methods Enzymol. 77, 50-59.

Pompella, A., Visvikis, A., Paolicchi, A., De Tata, V., Casini, A.F., 2003. The changing faces of glutathione, a cellular protagonist. Biochem. Pharmacol. 66, 1499-1503.

Potter, D.W., Finch, L., Udinsky, J.G., 1995. Glutathione content and turnover in rat tissues. Toxicol. Appl. Pharmacol. 135, 185-191.

Randerath, K., Reddy, M.V., Gupta, R.C., 1981. 32P-Labeling test for DNA damage. Proc. Natl. Acad. Sci. U.S.A. 78, 6126-6129.

Reddy, S.P., Mossman, B.T., 2002. Role and regulation of Activator Protein-1 in toxicant-induced responses of the lung. Am. J. Physiol. Lung Cell Mol. Physiol. 283, L1161-1178.

Reed, C.J., Robinson, D.A., Lock, E.A., 2003. Antioxidant status of the rat nasal cavity. Free Radic. Biol. Med. 34, 607-615.

Reliene, R., Schiestl, R.H., 2006. Glutathione depletion by buthionine sulfoximine induces DNA deletions in mice. Carcinogenesis 27, 240-244.

Renne, R.A. , Giddens, W.E. , Boorman, G.A., Kovatch, R., Haseman, J.E., Clarke, W. J., 1986. Nasal cavity neoplasia in F344/N rats and (C57BL/6 x C3H)F1 mice inhaling propylene oxide for up to two years. J. Natl. Cancer Inst. 77, 573-582.

Ríos-Blanco, M.N., Faller, T.H., Nakamura, J., Kessler, W., Kreuzer, P.E., Ranasinghe, A., Filser, J.G., Swenberg, J.A., 2000. Quantitation of DNA and hemoglobin adducts and apurinic/apyrimidinic sites in tissues of F344 rats exposed to propylene oxide by inhalation. Carcinogenesis 21, 2011-2018.

Ríos-Blanco, M.N., Plná, K., Faller, T., Kessler, W., Hakansson, K., Kreuzer, P.E., Ranasinghe, A., Filser, J.G., Segerbäck, D., Swenberg, J.A., 1997. Propylene oxide: mutagenesis, carcinogenesis and molecular dose. Mutat. Res. 380, 179-197.

Ríos-Blanco, M.N., Ranasinghe, A., Lee, M.S., Faller, T., Filser, J.G., Swenberg, J.A., 2003a. Molecular dosimetry of N7-(2-hydroxypropyl)guanine in tissues of F344 rats after inhalation exposure to propylene oxide. Carcinogenesis 24, 1233-1238.

Ríos-Blanco, M.N., Ranasinghe, A., Upton, P., Lee, M.S., Filser, J.G., Swenberg, J.A., 2002. Exposure-dependent accumulation of N-(2-hydroxypropyl) valine in hemoglobin of F344 rats exposed to propylene oxide by the inhalation route. J. Chromatogr. B Analyt. Technol. Biomed. Life Sci. 778, 383-391.

Ríos-Blanco, M.N., Yamaguchi, S., Dhawan-Robl, M., Kessler, W., Schoonhoven, R., Filser, J.G., Swenberg, J.A., 2003b. Effects of Propylene oxide exposure on rat nasal respiratory cell proliferation. Toxicol. Sci. 75, 279-288.

Rowe, V.K., Hollinsworth, R.L., Oyen, F., McCollister, D.D., Spencer, H.C., 1956. Toxicity of propylene oxide determined on experimental animals. Arch. ind. Health 13, 228-236.

Ruddick, J.A., 1972. Toxicology, metabolism, and biochemistry of 1,2-propanediol. Toxicol. Appl. Pharmacol. 21, 102-111.

Sachs, L., 1997. Angewandte Statistik—Anwendung statistischer Methoden. Springer Verlag, Berlin.

Schmidbauer, R., 1997. Toxikokinetik von Propen und Propenoxid bei Maus und Ratte. In Dissertation an der Fakultät für Chemie, Biologie und Geowissenschaften der Technischen Universität München.

Segerbäck, D., Osterman-Golkar, S., Molholt, B., Nilsson, R., 1994. *In vivo* tissue dosimetry as a basis for cross-species extrapolation in cancer risk assessment of propylene oxide. Regul. Toxicol. Pharmacol. 20, 1-14.

Segerbäck, D., Plná, K., Faller, T., Kreuzer, P.E., Hakansson, K., Filser, J.G., Nilsson, R., 1998. Tissue distribution of DNA adducts in male Fischer rats exposed to 500 ppm of propylene oxide: quantitative analysis of 7-(2-hydroxypropyl)guanine by 32P-postlabelling. Chem. Biol. Interact. 115, 229-246.

Shaulian, E., Karin M., 2001. AP-1 in cell proliferation and survival. Oncogene 20, 2390-2400.

Shaulian, E., Karin, M., 2002. AP-1 as a regulator of cell life and death. Nat. Cell Biol. 4, E131-E136.

Shukla, A., Flanders, T., Lounsbury, K.M., Mossman, B.T., 2004. The gamma-glutamylcysteine synthetase and glutathione regulate asbestos-induced expression of activator protein-1 family members and activity. Cancer Res. 64, 7780-7786.

Slater, A.F., Stefan, C., Nobel, I., van den Dobbelsteen, D.J., Orrenius, S., 1995. Signalling mechanisms and oxidative stress in apoptosis. Toxicol. Lett. 82-83, 149-153.

Snyder, C.A., Solomon, J.J., 1993. The extent and persistence of binding to respiratory mucosal DNA by inhaled tritiated propylene oxide. Cancer Lett. 72, 157-161.

Solomon, J.J., Mukai, F., Fedyk, J., Segal, A., 1988. Reactions of propylene oxide with 2'-deoxynucleosides and in vitro with calf thymus DNA. Chem. Biol. Interact. 67, 275-294.

St. Clair, M.B., Gross, E.A., Morgan, K.T., 1990. Pathology and cell proliferation induced by intra-nasal instillation of aldehydes in the rat: comparison of glutaraldehyde and formaldehyde. Toxicol. Pathol. 18, 353-361.

Steinkraus, V., Hausen, B.M., 1994. Contact allergy to propylene oxide. Contact Dermatitis 31, 120.

Svensson, K., Olofsson, K., Osterman-Golkar, S., 1991. Alkylation of DNA and hemoglobin in the mouse following exposure to propene and propylene oxide. Chem. Biol. Interact. 78, 55-66.

Svensson, K., Osterman-Golkar, S., 1984. Kinetics of metabolism of propene and covalent binding to macromolecules in the mouse. Toxicol. Appl. Pharmacol. 73, 363-372.

Tormos, C., Javier Chaves, F., Garcia, M.J., Garrido, F., Jover, R., O'Connor, J.E., Iradi, A., Oltra, A., Oliva, M.R., Sáez, G.T., 2004. Role of glutathione in the induction of apoptosis and c-fos and c-jun mRNAs by oxidative stress in tumor cells. Cancer Lett. 208, 103-113.

Valko, M., Rhodes, C.J., Moncol, J., Izakovic, M., Mazur, M., 2006. Free radicals, metals and antioxidants in oxidative stress-induced cancer. Chem. Biol. Interact. 160, 1-40.

van Ketel, W.G., 1979. Contact dermatitis from propylene oxide. Contact Dermatitis, 5, 191-192.

Vogel, E.W., Nivard, M.J.M., 1997. The response of germ cells to ethylene oxide, propylene oxide, propylene imine and methyl methanesulfonate is a matter of cell stage-related repair. Environ. Mol. Mutagen. 29, 124-135.

Vogel, E.W., Nivard, M.J.M., 1998. Genotoxic effects of inhaled ethylene oxide, propylene oxide and butylenes oxide on germ cells: sensitivity of genetic endpoints in relation to dose and repair status. Mutat. Res. 405, 259-271.

Walpole, A.L., 1958. Carcinogenic action of alkylating agents. Ann. N. Y. Acad. Sci. 68, 750-761.

Weil, C.S., Condra, N., Haun, C., Striegel, J.A., 1963. Experimental Carcinogenicity and acute toxicity of representative epoxides. Am. Ind. Hyg. Assoc. J., 24, 305-325.

WHO, World Health Organization, 1985. Propylene oxide. Environ. Health Crit. 56, 1-53.

Young, J.T., 1981. Histopathologic examination of the rat nasal cavity. Fundam. Appl. Toxicol. 1, 309-312.

Zuwei, X., Ning, Z., Yu, S., Kunlan, L., 2001. Reaction-controlled phase-transfer catalysis for propylene epoxidation to propylene oxide. Science 292, 1139-1141.